

Alma Mater Studiorum Università di Bologna  
Archivio istituzionale della ricerca

Ruthenium tris(bipyridine) complexes: Interchange between photons and electrons in molecular-scale devices and machines

This is the final peer-reviewed author's accepted manuscript (postprint) of the following publication:

*Published Version:*

Balzani V., Ceroni P., Credi A., Venturi M. (2021). Ruthenium tris(bipyridine) complexes: Interchange between photons and electrons in molecular-scale devices and machines. COORDINATION CHEMISTRY REVIEWS, 433, 1-23 [10.1016/j.ccr.2020.213758].

*Availability:*

This version is available at: <https://hdl.handle.net/11585/812769> since: 2021-08-31

*Published:*

DOI: <http://doi.org/10.1016/j.ccr.2020.213758>

*Terms of use:*

Some rights reserved. The terms and conditions for the reuse of this version of the manuscript are specified in the publishing policy. For all terms of use and more information see the publisher's website.

This item was downloaded from IRIS Università di Bologna (<https://cris.unibo.it/>).  
When citing, please refer to the published version.

(Article begins on next page)

This is the final peer-reviewed accepted manuscript of:

**Balzani, V.; Ceroni, P.; Credi, A.; Venturi, M. Ruthenium Tris(Bipyridine) Complexes: Interchange between Photons and Electrons in Molecular-Scale Devices and Machines. Coordination Chemistry Reviews 2021, 433, 213758**

The final published version is available online at:  
<https://doi.org/10.1016/j.ccr.2020.213758>

#### Terms of use:

Some rights reserved. The terms and conditions for the reuse of this version of the manuscript are specified in the publishing policy. For all terms of use and more information see the publisher's website.

*This item was downloaded from IRIS Università di Bologna (<https://cris.unibo.it/>)*

***When citing, please refer to the published version.***

# Ruthenium tris(bipyridine) complexes: interchange between photons and electrons in molecular-scale devices and machines

Vincenzo Balzani,<sup>1\*</sup> Paola Ceroni,<sup>1\*</sup> Alberto Credi,<sup>2,3\*</sup> Margherita Venturi<sup>1\*</sup>

<sup>1</sup> Dipartimento di Chimica “G. Ciamician”, Università di Bologna, via Selmi 2, 40126 Bologna, Italy

<sup>2</sup> Dipartimento di Chimica Industriale “Toso Montanari”, Università di Bologna, viale del Risorgimento 4, 40136 Bologna, Italy

<sup>3</sup> CLAN-Center for Light Activated Nanostructures, ISOF-CNR, via Gobetti 101, 40129 Bologna, Italy

E-mail: [vincenzo.balzani@unibo.it](mailto:vincenzo.balzani@unibo.it); [paola.ceroni@unibo.it](mailto:paola.ceroni@unibo.it); [alberto.credi@unibo.it](mailto:alberto.credi@unibo.it); [margherita.venturi@unibo.it](mailto:margherita.venturi@unibo.it)

## Abstract

This review deals with a very peculiar molecule,  $[\text{Ru}(\text{bpy})_3]^{2+}$  (bpy: 2,2'-bipyridine), and its interaction with photons and electrons. We summarize the properties that make  $[\text{Ru}(\text{bpy})_3]^{2+}$  and related compounds a unique family of “clever” molecules which find application as components of chemical species capable of processing optical and electrical signals to perform a variety of interesting functions. Examples discussed in the article, that showcase the realization of these concepts with molecular and supramolecular systems, include molecular wires, switches, antennas and mechanical machines.

Keywords: dendrimer; electrochemistry; photochemistry; rotaxane; supramolecular chemistry

## Table of Contents

1. Introduction	3
1.1. Properties of electronic excited states	5
1.2. Structure, bonding, and excited states of Ru(II) polypyridine complexes	7
1.3. Connection between photons and electrons	10
1.4. Properties of $[\text{Ru}(\text{bpy})_3]^{2+}$	11
1.5. Interchange between photons and electrons with $[\text{Ru}(\text{bpy})_3]^{2+}$	13
2. Photoinduced energy or electron transfer processes in supramolecular dyads and triads	16
2.1. Wires for photoinduced energy and electron transfer processes	16
2.2. Shape-persistent macrocyclic bridges	19
2.3. Switching electron and energy transfer processes	21
2.4. Energy reservoir	23
3. Dendrimers	26
3.1. Dendrimers with a $[\text{Ru}(\text{bpy})_3]^{2+}$ -type complex in the core	28
3.2. Dendrimers with Ru polypyridine-type complexes at their periphery	30
3.3. Dendrimers with Ru polypyridine-type complexes as the branching elements	32
3.4. A proton-driven assembly of a luminescent dendrimer with a Ru bpy-type complex	38
4. Molecular machines	39
4.1. Basic concepts	39
4.2. Photoinduced energy transfer	40
4.3. Photoinduced electron transfer	41
4.4. Ligand photodissociation	48
5. Conclusion	51
6. References	52

## 1. Introduction

Chemical reactions are the core of chemistry. Most reactions take place by thermal excitation (heat) causing the conversion of a reagent into a product. In the case of metal complexes, thermal reactions in solution often cause replacement of a ligand by a solvent molecule or even the complete disruption of the complex. The same result can often be obtained upon light excitation [1] or electrochemical reduction/oxidation [2].

Nowadays photons and electrons are indeed more and more commonly used to cause chemical reactions. Light excitation of a metal complex never causes the immediate disruption of the complex, but the formation of electronically excited states that undergo, usually in a very short time, physical deactivation or an irreversible chemical reaction. In the same way, electrochemical reduction/oxidation does not cause immediate disruption of the complex, but yields a one-electron oxidized/reduced complex that, in most cases, undergoes irreversible fast secondary reactions.

$[\text{Ru}(\text{bpy})_3]^{2+}$  (bpy: 2,2'-bipyridine) exhibits a unique combination of chemical stability in the ground state, in its lowest excited state  $^*[\text{Ru}(\text{bpy})_3]^{2+}$ , and in the one-electron reduced  $[\text{Ru}(\text{bpy})_3]^+$  and oxidized  $[\text{Ru}(\text{bpy})_3]^{3+}$  forms [3]. This quite unusual combination allows the use of  $[\text{Ru}(\text{bpy})_3]^{2+}$  in a variety of processes in which photons and electrons can be interchanged [4, 5]. This is the reason why in the past 50 years many researchers have been attracted by  $[\text{Ru}(\text{bpy})_3]^{2+}$ , as well as by some hundreds of its derivatives, for a variety of purposes [6, 7] (Figure 1).

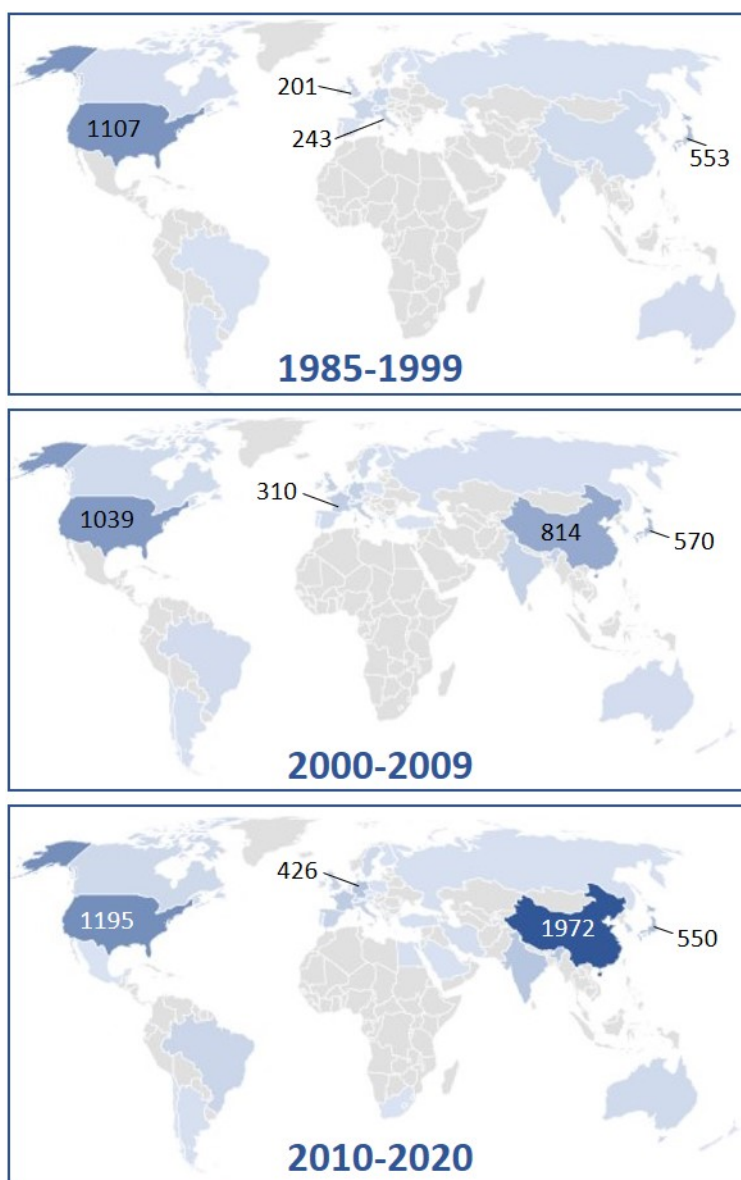


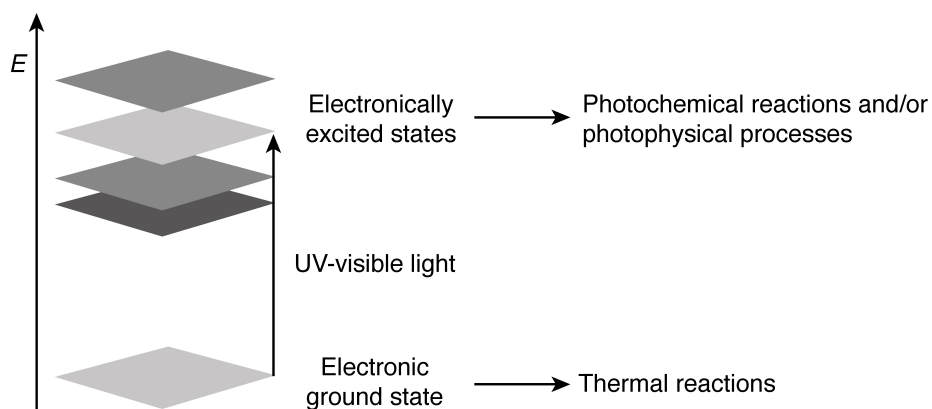
**Figure 1.** Time evolution and geographical distribution of papers on  $[\text{Ru}(\text{bpy})_3]^{2+}$ -type complexes. The number of papers published for the first four countries in order of published papers are reported. Web of Science: search on <ruthenium> and (bipyridine or oligopyridine or polypyridine).

Research in this field has directly or indirectly contributed to the development of traditional and novel fields of chemistry: photochemistry, electrochemistry, photophysics, absorption and emission spectroscopy, electron transfer, energy transfer, photocatalysis, chemi- and electrochemiluminescence, solar energy conversion, supramolecular photochemistry, luminescent sensors, polynuclear metal complexes, photoinduced charge-separation devices, light-active dendrimers, and

light-powered molecular devices and machines. No doubt,  $[\text{Ru}(\text{bpy})_3]^{2+}$  has been one of the most influential molecules for the development of chemistry in the last five decades.

### 1.1. Properties of electronic excited states

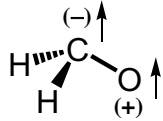
Light excitation with a photon of suitable energy promotes a molecule from its *ground state* to an electronically *excited state* (Figure 2). The ground state of the molecule is responsible for the dark (thermal) reactions, whereas the excited states are responsible for the photochemical reactions and the photophysical deactivation processes [3].



**Figure 2.** Light excitation with a photon of suitable energy promotes a molecule from its *ground state* to an electronically *excited state*, opening a new dimension to chemistry and physics. Adapted from ref. [3].

Light excitation modifies the electronic structure of a molecule. Therefore, each excited state is a *new chemical species* with its own chemical and physical properties, different from the properties of the ground state [3]. This is clearly shown by Table 1 that compares some properties of the ground state and the lowest excited state of formaldehyde [8]. Clearly, photochemistry opens a new dimension to chemistry.

**Table 1.** Comparison between ground and excited state properties of formaldehyde [8].

	ground state	lowest excited state
	$\begin{array}{c} \text{H} \\ \diagdown \\ \text{C}=\text{O} \\ \diagup \\ \text{H} \end{array}$	
energy (kcal/mol)	0	+ 76
geometry	planar	pyramidal
magnetism	diamagnetic	paramagnetic
dipole moment (D)	2.3	1.3
$r_{\text{CO}}$ (Å)	1.22	1.31
$\nu_{\text{CO}}$ ( $\text{cm}^{-1}$ )	1745	1180
lifetime (s)	$\infty$	$< 10^{-3}$

The electronic excited states, because of their higher energy content, are transient species that must undergo fast deactivation. Intramolecular deactivation may occur essentially in three ways (Figure 3): (i) a chemical reaction leading to a product, e.g., an isomer; (ii) emission of light, luminescence; (iii) radiationless deactivation to the ground state [3].

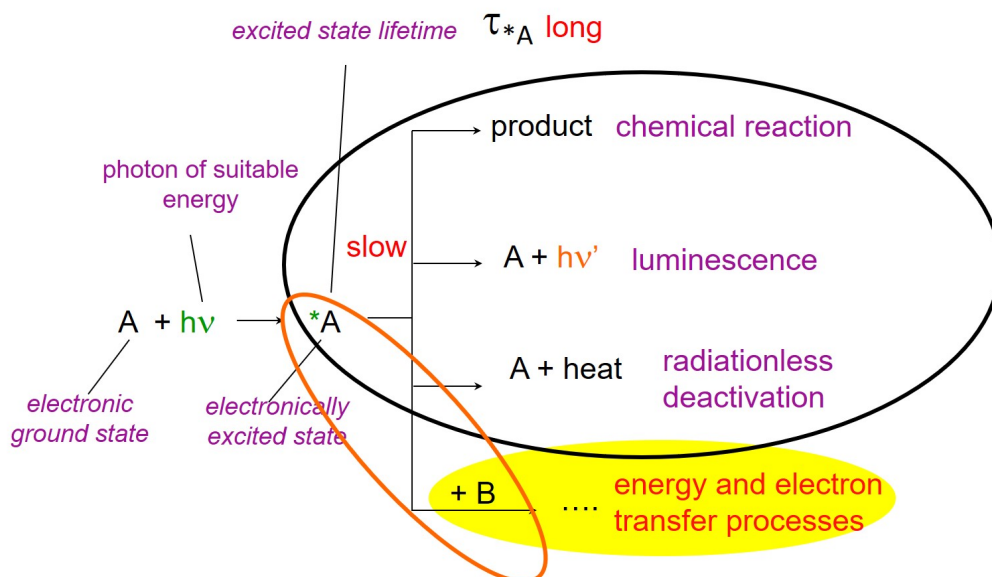




**Figure 3.** Scheme of the processes that can take place after photoexcitation. The ellipse indicates that when the intramolecular deactivation processes are slow, the excited state lifetime may be long enough to allow encounters of the excited state with other species giving rise to energy and electron transfer processes

The lifetime of the excited state,  $\tau_{*A}$ , depends on the rates of the three concurrent deactivation processes. When these processes are slow, the excited state lifetime is long so that the excited state has a chance to go around in the solution and encounter another species, B, giving rise to energy- or electron-transfer processes (Figure 3) [3].

As we will see later, not only the excited state has an extra amount of energy compared with the ground state but, most important, the excited state is both a better reductant and a better oxidant than the corresponding ground state.

## 1.2. Structure, bonding, and excited states of Ru(II) polypyridine complexes

$\text{Ru}^{2+}$  in octahedral complexes is a  $d^6$  system and the polypyridine ligands are usually colorless molecules with  $\sigma$  donor orbitals on the nitrogen atoms and  $\pi$  donor and  $\pi^*$  acceptor orbitals delocalized to some extent on the aromatic rings.  $[\text{Ru}(\text{bpy})_3]^{2+}$  as well as most of the  $[\text{Ru}(\text{LL})_3]^{2+}$  complexes (LL = bidentate polypyridine ligand), exhibit a  $D_3$  symmetry [9], but for our purposes we can assume an octahedral symmetry.

In a single-configuration one-electron picture of the excited states in octahedral symmetry (Figure 4), an electronic transition from a  $\pi_M$  metal orbital to the  $\pi^*_L$  ligand orbitals forms metal-to-ligand charge transfer (MLCT) excited states, whereas transition of an electron from  $\pi_M$  to  $\sigma^*_M$  orbitals leads to metal-centered (MC) excited states. Ligand-centered (LC) excited states are obtained by promotion of an electron from  $\pi_L$  to  $\pi^*_L$ . All these excited states may be considered to exhibit singlet or triplet multiplicity, although in MC and MLCT excited states spin-orbit coupling causes singlet-triplet mixing [3].

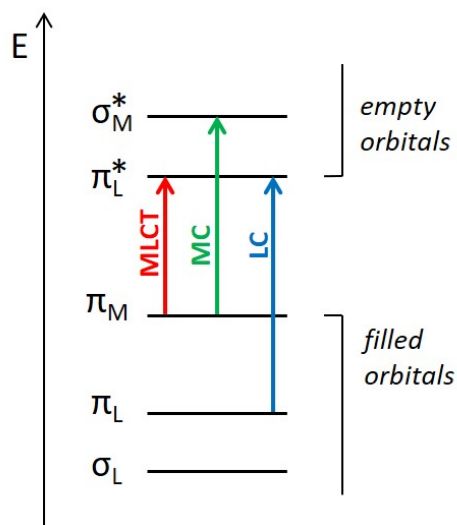


**Figure 4.** Simplified molecular orbital diagram for Ru(II) polypyridine complexes showing the types of electronic transitions occurring at low energies in octahedral symmetry.

According to the well-known Kasha's rule [3], only the lowest excited state of a molecule and the closely lying states that can be populated because of the Boltzmann equilibrium distribution may play a role in determining the photochemical and photophysical behavior of a molecule. This is even more true for metal complexes because even the spin-forbidden deactivation processes of the high energy levels are facilitated by some spin-orbit coupling. It is also known that for  $d^6$  octahedral complexes the MC excited states are strongly displaced with respect to the ground-state geometry along the metal-ligand vibration coordinates. Therefore, when the lowest excited state of a complex is MC, fast radiationless deactivation to the ground state and/or ligand dissociation reactions take place (Figure 5a). In such a case, the excited-state lifetime is very short at room temperature and no luminescence can be observed. Under such conditions, very rarely bimolecular reactions can take place. The LC and MLCT excited states of octahedral complexes are usually not strongly distorted compared to the ground-state geometry. Therefore, when the lowest excited state is LC or MLCT (Figure 5b) fast radiationless decay to the ground state does not occur and luminescence can usually be observed. Because of the larger spin-orbit coupling effect, the rate constant for radiative deactivation is somewhat higher for  $^3\text{MLCT}$  than for  $^3\text{LC}$ . It follows that the  $^3\text{LC}$  excited states are longer lived in a rigid matrix at low temperature and that the  $^3\text{MLCT}$  excited states are more likely to exhibit luminescence in fluid solution at room temperature.

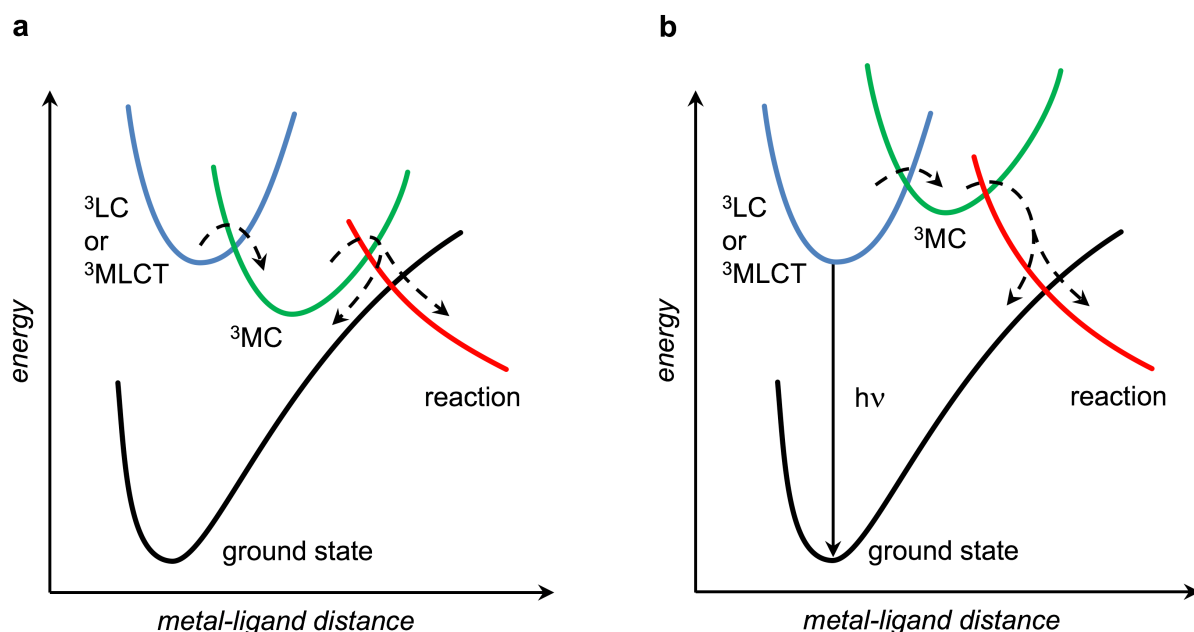


**Figure 5.** Schematic representation of two limiting cases for the relative positions of  $^3\text{MC}$  and  $^3\text{LC}$  (or  $^3\text{MLCT}$ ) excited states. Adapted from ref. [9].

From the above discussion, it follows that the excited-state properties of a complex are related to the orbital nature of its lowest excited state and to their energy ordering. The energy positions of the MC, MLCT, and LC excited states depend essentially on the ligand field strength, the redox properties of the metal and the ligands, and intrinsic properties of the ligands, respectively [10]. Thus, for complexes of the same metal ion the excited state energy ordering and the orbital nature of the lowest excited state can be controlled by the choice of the ligands [6] and it is possible, at least to a certain degree, to design complexes that exhibit the desired properties.

For Ru(II) polypyridine complexes, the lowest excited state is usually a  $^3\text{MLCT}$  level which undergoes relatively slow radiationless deactivation because of the high energy gap with the ground state. Therefore, it exhibits luminescence and a relatively long lifetime. If the three bidentate ligands are different, the lowest  $^3\text{MLCT}$  is obtained by promoting an electron from the metal  $\pi_{\text{M}}$  orbital to the  $\pi_{\text{L}}^*$  orbital of the ligand that is easier to reduce. The same  $\pi_{\text{L}}^*$  orbital, indeed, is usually involved in the one-electron reduction process [6].

### 1.3. Connection between photons and electrons

A connection between light excitation and redox properties of molecules was first reported long ago by Giacomo Ciamician [11], who observed that light excitation facilitates redox reactions. Nowadays we know why: the electronically excited states of molecules are *both* better electron acceptors *and* better electron donors than the ground state species [3]. This is schematically shown in the orbital diagram of Figure 6. Usually, absorption of light promotes an electron from a lower energy to a higher energy orbital. The promoted electron can be more easily removed, so that the excited state has a smaller ionization potential than the ground state. Together, a low-lying vacancy is formed that can accept an electron, which means that the excited state has also a higher electron affinity than the ground state.

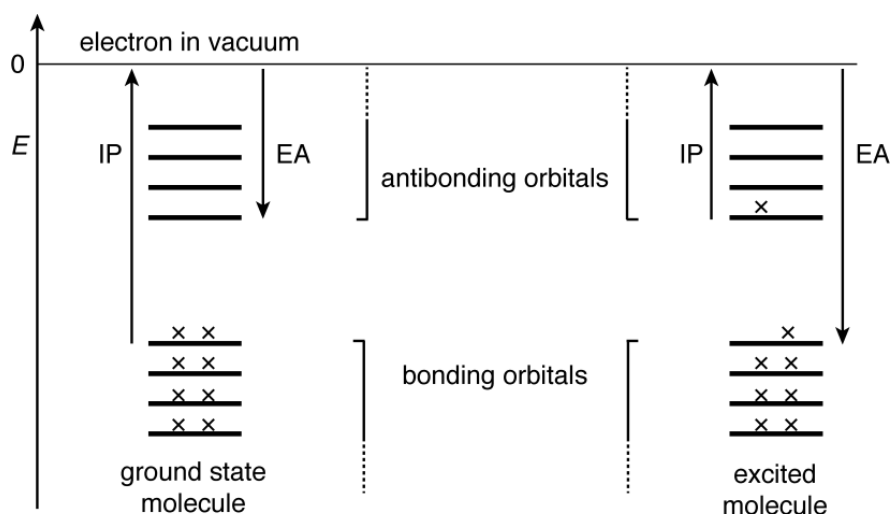


**Figure 6.** Scheme based on molecular orbitals elucidating why an excited state is *both* a better electron donor *and* a better electron acceptor than the ground state [3].

Therefore, light excitation is by itself an unusual redox process resulting in a “product” capable to play the dual role of an oxidant and a reductant.

Quantitatively, the unusual excited state redox properties depend on the extra amount of energy of the excited state. For a thermally equilibrated excited state and reversible redox reactions, the excited state redox potentials can be defined by equations 1 and 2 [3]:

$$E^0(A^+/*A) = E^0(A^+/A) - E_{00}(*A/A) \quad (1)$$

$$E^0(*A/A^-) = E^0(A/A^-) + E_{00}(*A/A) \quad (2)$$

in which  $E_{00}(*A/A)$  is the one-electron potential equivalent to the electronic energy of the excited state (i.e., the difference between the zero vibrational levels of ground and excited state). It should be noted that  $E_{00}(*A/A)$  concerns the *reactive* excited state, which most often does not coincide with the excited state directly populated by light absorption. On the basis of the above equations, for a reversible reaction



the free energy change is given by:

$$\Delta G_{et}^0 = N_A \{ e[E(B^+/B) - E(A/A^-)] + w(A^-B^+) \} - E_{00}(*A/A) \quad (4)$$

in which  $N_A$  is the Avogadro constant,  $e$  is the elementary charge ( $e = 1.602 \times 10^{-19}$  C) and  $w$  is the electrostatic work term accounting for Coulomb interactions between the reaction partners after electron transfer (a term that can be neglected, to a first approximation). When the processes involved are irreversible, the potential values are not available; sometimes they can be estimated from other parameters [12], but it is difficult to forecast whether the actual electron-transfer process will take place under the experimental condition used.

#### 1.4. Properties of $[Ru(bpy)_3]^{2+}$

We can use  $[Ru(bpy)_3]^{2+}$  to illustrate the above concepts and appreciate why this complex can be used in a variety of processes and applications.

In solution,  $[Ru(bpy)_3]^{2+}$  is stable toward ligands dissociation [6] both in the dark and upon light excitation (some members of its family, however, may undergo ligand photodissociation, see e.g. Section 4.4) and exhibits a fully reversible redox behavior, both in oxidation and reduction [13] (Figure 7).

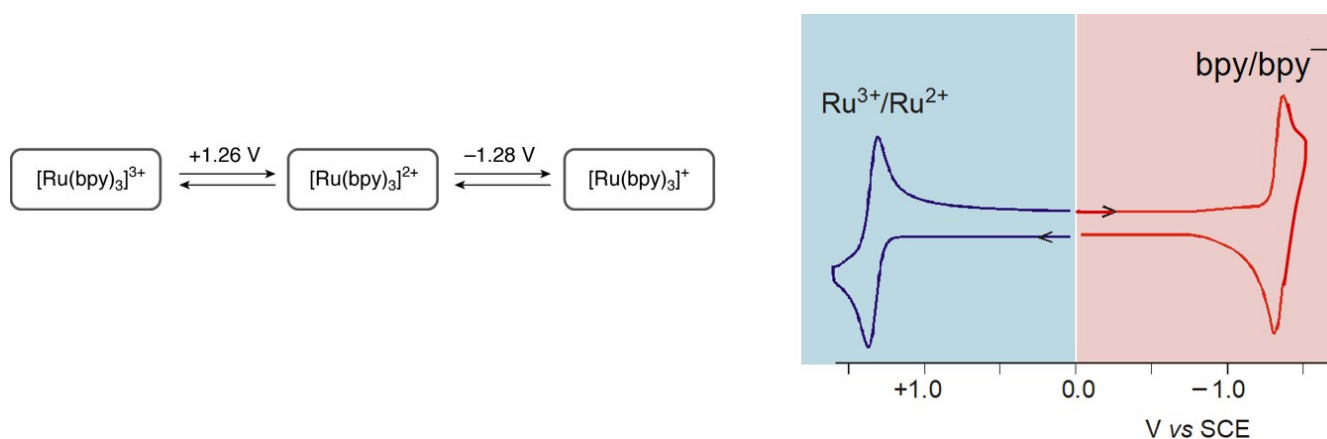


**Figure 7.**  $[\text{Ru}(\text{bpy})_3]^{2+}$  does not undergo ligand release in solution at room temperature and exhibits a fully reversible redox behavior showing that the oxidized and reduced species do not undergo fast ligand release. Cyclic voltammetric curves recorded in acetonitrile solution.

The absorption and emission spectra of  $[\text{Ru}(\text{bpy})_3]^{2+}$  are shown in Figure 8.

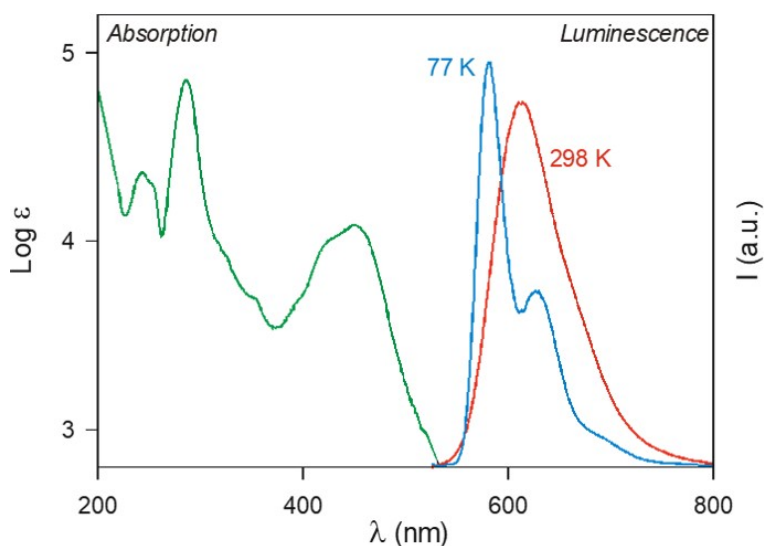


**Figure 8.** The absorption (298 K) and emission spectra (298 and 77 K) of  $[\text{Ru}(\text{bpy})_3]^{2+}$  in acetonitrile [14].

The bands in the UV region at 185 nm (not shown) and 285 nm are present also in the spectrum of protonated bipyridine and thus assigned to spin-allowed LC  $\pi \rightarrow \pi^*$  transitions [6]. The two intense bands at 240 and 450 nm are assigned to spin-allowed MLCT  $d \rightarrow \pi^*$  transitions. The shoulders at 322 and 344 nm might be due to MC transitions. In the tail of the absorption spectrum (in an ethanol-

methanol glass at 77 K) a shoulder is present at about 550 nm ( $\epsilon \sim 600 \text{ M}^{-1} \text{ cm}^{-1}$ ) [15]. Such an absorption feature is assigned to spin-forbidden MLCT transitions.

Excitation of  $[\text{Ru}(\text{bpy})_3]^{2+}$  in any of its absorption bands leads to a luminescence emission (Figure 8) that is attributed to the lowest excited state, a triplet metal-to-ligand excited state,  $^3\text{MLCT}$ . In the following, as well as in the scheme of Figure 9, the lowest excited state is indicated by  $^*[\text{Ru}(\text{bpy})_3]^{2+}$  and the excited states reached by light excitation in all the intense absorption bands are cumulatively indicated by  $^{**}[\text{Ru}(\text{bpy})_3]^{2+}$ .

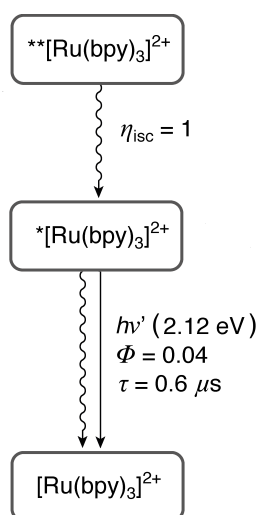


**Figure 9.** Schematic representation of light excitation and light emission of  $[\text{Ru}(\text{bpy})_3]^{2+}$ .  $^{**}\text{Ru}(\text{bpy})_3]^{2+}$  stays for the ensemble of spin allowed excited states corresponding to the intense bands of the absorption spectrum (Figure 8) and  $^*\text{Ru}(\text{bpy})_3]^{2+}$  is the lowest spin forbidden excited state  $^3\text{MLCT}$  responsible for the luminescence emission (Figure 8).

The decay of the upper excited states to the lowest one takes place with unitary efficiency in the **sub-picosecond** time scale. In aqueous solution, the lowest excited state lies 2.12 eV above the ground state, shows a lifetime of 0.6 microseconds and an emission quantum yield of 0.04.

### 1.5. Interchange between photons and electrons with $[\text{Ru}(\text{bpy})_3]^{2+}$

As we have seen above, the extra amounts of energy of the excited state compared with the ground state can be used both in oxidation and reduction processes, so that the excited state is both a better oxidant and a better reductant than the ground state.

Figure 10 summarizes the energy relations between the various forms of  $[\text{Ru}(\text{bpy})_3]^{2+}$ . In this system there are four species,  $[\text{Ru}(\text{bpy})_3]^{2+}$ ,  $^*[\text{Ru}(\text{bpy})_3]^{2+}$ ,  $[\text{Ru}(\text{bpy})_3]^+$ , and  $[\text{Ru}(\text{bpy})_3]^{3+}$  that can be interconverted by using light or electric inputs. Each one of these species exhibits specific absorption bands that allow monitoring their formation and disappearance.

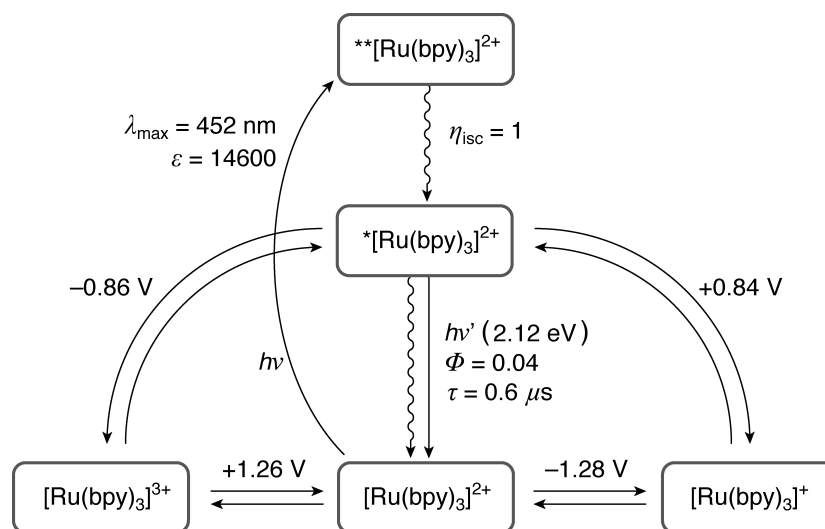
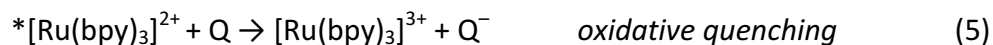


**Figure 10.** Properties of  $[\text{Ru}(\text{bpy})_3]^{2+}$  relevant to electron transfer processes.  $^{**}[\text{Ru}(\text{bpy})_3]^{2+}$  is the spin-allowed excited state reached upon light absorption and  $^*[\text{Ru}(\text{bpy})_3]^{2+}$  is the lowest spin-forbidden excited state ( $^3\text{MLCT}$ ), responsible for the luminescence. Reduction potentials are *versus* NHE. Adapted from ref. [3].

Light excitation in the intense absorption band in visible region ( $\lambda_{\text{max}}=452 \text{ nm}$ ,  $\epsilon_{\text{max}} 14600 \text{ M}^{-1} \text{ cm}^{-1}$ ) leads to the lowest spin-allowed metal-to-ligand charge transfer ( $^1\text{MLCT}$ ) excited state ( $^{**}[\text{Ru}(\text{bpy})_3]^{2+}$ ), which undergoes very fast (picosecond time scale) intersystem crossing to the lowest  $^3\text{MLCT}$  excited state ( $^*[\text{Ru}(\text{bpy})_3]^{2+}$ ). As we have seen above, this excited state is stable toward ligand release and lives  $0.6 \mu\text{s}$ , long enough to encounter other solute molecules before undergoing radiative or radiationless physical deactivation. The extra energy available to  $^*[\text{Ru}(\text{bpy})_3]^{2+}$  amounts to  $2.12 \text{ eV}$  compared with the ground state, so that its reduction and oxidation potentials (equations 1 and 2), are  $+0.84$  and  $-$



0.86 V (vs NHE, in water). Clearly,  $^*[Ru(bpy)_3]^{2+}$  is both a good electron donor (reaction 5), and a good electron acceptor (reaction 6):



Potentially, the two processes are in competition, but usually, for a given Q, only one of them is thermodynamically allowed. When both are allowed, kinetic factors establish which of them wins the competition.

For reactions taking place in fluid solution between the  $^*[Ru(bpy)_3]^{2+}$  excited state and a solute Q (e.g., reactions 5 and 6, sometimes called dynamic quenching processes), the ratio of the excited state lifetime in the absence ( $\tau^0$ ) and presence ( $\tau$ ) of Q is given by equation 7, called the Stern-Volmer equation [3]:

$$\tau^0/\tau = 1 + \tau^0 k_q [Q] \quad (7)$$

in which  $k_q$  is the rate of the quenching process and the product  $\tau^0 k_q$  is named Stern-Volmer constant ( $k_{sv}$ ). The upper limit value of  $k_q$  is the diffusion rate constant ( $k_d$ ) in the solvent used. Assuming that the reaction occurs at its upper limit rate,  $k_q = k_d$ , equation 7 can be employed to evaluate the smallest concentration of quencher Q required to quench the luminescent excited state with a predetermined efficiency.

Figure 10 shows that  $[Ru(bpy)_3]^{2+}$  allows us to merge, mix and interchange photonic and electronic signals and can not only convert photons into electrons, but also electrons into photons. This complex has indeed been used in a variety of photoinduced electron transfer processes, but also in electrochemi-luminescence experiments to generate light by means of an electrochemical reaction, that is to convert an electron input into a photon output [16, 17]. With this complex we have even created an oscillating chemiluminescent system, that is an artificial firefly [18]. The oscillating Belousov–Zhabotinskii reaction consists in the oxidation of carboxylic acids by bromate ions catalyzed by  $[Fe(phen)_3]^{2+}$ . This reaction proceeds through a periodic rate fluctuation, which also causes a fluctuation in the concentration of the reduced and oxidized forms of the catalyst. When  $[Ru(bpy)_3]^{2+}$  replaces  $[Fe(phen)_3]^{2+}$ ,  $[Ru(bpy)_3]^{3+}$  can be reduced by carboxylic acids to yield the luminescent excited state of  $[Ru(bpy)_3]^{2+}$  and an oscillating chemiluminescence emission.

Electron and photons are indeed the two most important means that enable to stimulate molecules and process information [5]. We have shown that because of its properties  $[\text{Ru}(\text{bpy})_3]^{2+}$  can play, alone, the role of a 4-to-2 encoder and a 2-to-4 decoder [19]. For example, we can compress four distinct writing inputs, one photonic (excitation at 450 nm) and three electronic inputs (potential difference of +1.4 V vs SCE, potential difference of -1.4 V vs SCE and square wave potential between the previous two potential values), into combinations of only two (photonic) reading outputs, namely absorption at 530 nm and emission intensity at 620 nm. When necessary, reset of the system can be obtained. For more details, the reader can refer to the original paper [19].

Many examples of applications of the unique properties of  $[\text{Ru}(\text{bpy})_3]^{2+}$  are illustrated in the following sections.

## 2. Photoinduced energy or electron transfer processes in supramolecular dyads and triads

### 2.1. Wires for photoinduced energy and electron transfer processes

**Energy transfer.** Electronic energy transfer over long distances and/or along predetermined directions can be obtained by bridging donor and acceptor components with a rigid spacer. The ruthenium oligopyridine complexes are among the most investigated systems either as donor or as acceptor units. Indeed, the photophysical properties of these complexes are very appropriate to such an application: they are luminescent also in air-equilibrated solution with quite long excited state lifetimes compared to fluorescent organic species. Therefore, the occurrence of energy transfer can be monitored by quenching and/or sensitization experiments with continuous and pulsed excitation techniques.

The prototypical example is constituted by the  $[\text{Ru}(\text{bpy})_3]^{2+}-(\text{ph})_n-[\text{Os}(\text{bpy})_3]^{2+}$  compounds (ph = 1,4-phenylene; n = 2-5) [20, 21]: excitation of the  $[\text{Ru}(\text{bpy})_3]^{2+}$  unit is followed by electronic energy transfer from the lowest  $^3\text{MLCT}$  state to populate the lowest  $^3\text{MLCT}$  of the  $[\text{Os}(\text{bpy})_3]^{2+}$  unit, as shown by the sensitized emission of the latter. A schematic energy level diagram is reported in Figure 11. The lowest energy level of the polyphenylene bridge,  $T_1$ , decreases slightly as the number of phenylene units increases, but in all cases lies above the  $[\text{Ru}(\text{bpy})_3]^{2+}$   $^3\text{MLCT}$  and  $[\text{Os}(\text{bpy})_3]^{2+}$   $^3\text{MLCT}$  levels. As expected, the rate of energy transfer decreases with increasing the length of the bridge (Figure 12) according to a superexchange mechanism, in which the electronic coupling of the donor and acceptor units is

mediated by mixing the initial and final states of the system with virtual, high energy states of the bridge.

The effect of the conjugation of the bridge is clearly evident by comparison of the  $[\text{Ru}(\text{bpy})_3]^{2+}-(\text{ph})_3-$   $[\text{Os}(\text{bpy})_3]^{2+}$  with the corresponding molecular wire in which the central phenylene ring of the bridge is functionalized by two hexyl groups: the photoinduced electron-transfer process is 10 times slower, presumably because the solubilizing hexyl groups increase the twist angle between the phenylene units, thereby reducing electronic coupling between the two metal centers.

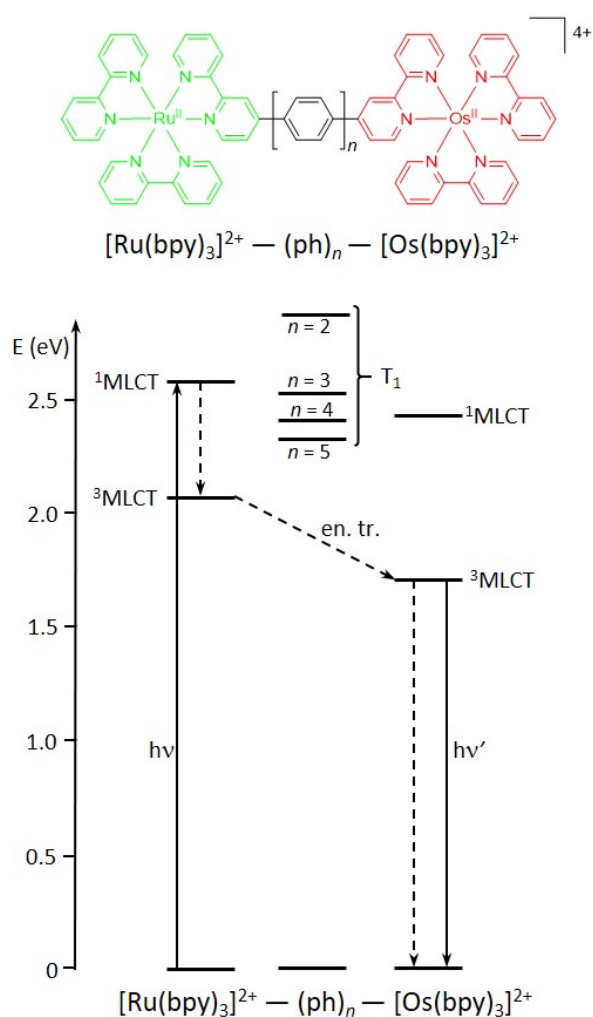


**Figure 11.** Energy level diagram for energy transfer in the  $[\text{Ru}(\text{bpy})_3]^{2+}-(\text{ph})_n-[\text{Os}(\text{bpy})_3]^{2+}$  compounds for bridges of different length ( $n = 2-5$ ) [21].

A closely related wire is represented by  $[\text{Ir}(\text{ppyF}_2)_2(\text{bpy})]^+-(\text{ph})_n-[\text{Ru}(\text{bpy})_3]^{2+}$  ( $\text{ppyF}_2 = (4',6'$ -difluoro)phenyl-pyridine) [22], where the Ir(III) complex is the donor and the Ru(II) complex is the acceptor. Upon excitation of the Ir(III) complex sensitized emission of the Ru(II) complex is observed, demonstrating the occurrence of the energy transfer process, but the rate is substantially independent from the length of the spacer (Figure 12). In this case, the  $T_1$  level of the bridge lies between the donor and acceptor level, at least for  $n = 2-5$ . Therefore, a hopping mechanism is operative, i.e. a sequential energy transfer from the donor to the bridge and finally to the acceptor.

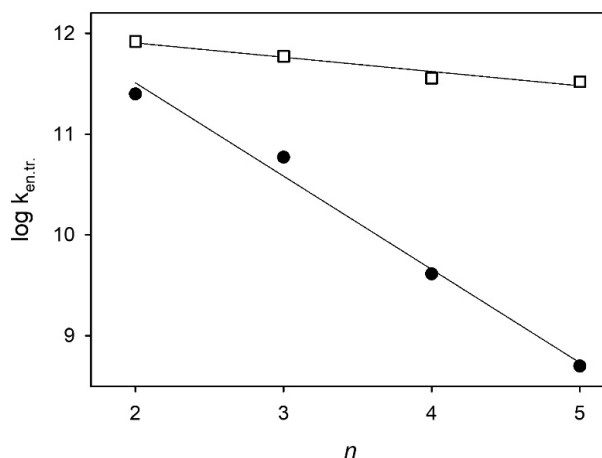


**Figure 12.** Distance-dependence of the electron transfer rate constant for the molecular wires  $[\text{Ru}(\text{bpy})_3]^{2+}-(\text{ph})_n-[\text{Os}(\text{bpy})_3]^{2+}$  (solid circles [21]) and  $[\text{Ir}(\text{ppyF}_2)_2(\text{bpy})]^+-(\text{ph})_n-[\text{Ru}(\text{bpy})_3]^{2+}$  (empty squares,[22]) with  $n = 2-5$ .

**Photoinduced electron transfer.** The minimum model of a wire for photoinduced electron transfer consists of an electron-donor (or acceptor) chromophore, an electron-acceptor (or donor) moiety and a bridge that controls their distance and electronic interactions (and therefore the rates and yields of the electron transfer).

In the  $[\text{Ru}(\text{bpy})_3]^{2+}-(\text{ph})_n-[\text{Os}(\text{bpy})_3]^{3+}$  compounds, obtained by chemical oxidation of the Os-based moiety of the previously discussed example (Figure 11), photoexcitation of the  $[\text{Ru}(\text{bpy})_3]^{2+}$  unit causes the transfer of an electron to the Os(III)-based one, followed by a rapid back electron transfer reaction from the  $[\text{Os}(\text{bpy})_3]^{2+}$  unit to the  $[\text{Ru}(\text{bpy})_3]^{3+}$  one.

A closely related study was reported on dyads  $[\text{Ru}(\text{phen})_2(\text{bpy})]^{2+}-(\text{ph})_n-[\text{Rh}(\text{bpy})_3]^{3+}$  with  $n = 1-3$  [23]. Upon selective excitation of the Ru(II)-based chromophoric unit, an electron transfer to the Rh(III)-based unit takes place, a process that is then followed by a back electron-transfer reaction. The rate constant for photoinduced electron transfer decreases exponentially with increasing metal-metal distance, as expected for a superexchange mechanism, with an attenuation factor  $\beta = 0.50 \text{ \AA}^{-1}$ , a value much lower than that found for rigid unsaturated bridges ( $0.8-1.2 \text{ \AA}^{-1}$ ).

The role of the spacer in mediating photoinduced and thermal (back) electron-transfer process is crucial [24].

In view of the conversion of light into chemical energy, the dyad-type systems suffer to a greater or lesser extent from rapid charge recombination and multicomponent systems were investigated to address this issue [Chapter 11 in ref. 3].

## 2.2. Shape-persistent macrocyclic bridges

It is worth considering the previously presented wires containing Ru(II) and Os(II)/Os(III) oligopyridine complexes connected by a linear oliphenylene bridge in comparison with the below reported examples in which the same metal complexes are linked by a shape persistent phenylacetylene macrocycle, **M**, which incorporates two bpy chelating units on opposite sides of its shape-persistent structure (Figure 13) [25].

**Energy transfer.** The absorption spectra of the dinuclear  $[(\text{bpy})_2\text{Ru}(\mathbf{M})\text{Os}(\text{bpy})_2]^{4+}$  complex in acetonitrile solution is equal to that of a 1:1 mixture of the homodinuclear  $[(\text{bpy})_2\text{Ru}(\mathbf{M})\text{Ru}(\text{bpy})_2]^{4+}$  and  $[(\text{bpy})_2\text{Os}(\mathbf{M})\text{Os}(\text{bpy})_2]^{4+}$  parent compounds and the electrochemical properties are those expected on the basis of their parent homodinuclear compounds [26]. For example, the oxidation processes of the Os(II)-and Ru(II)-based units take place at potential values very close to those reported for the respective mononuclear species, demonstrating that there is no appreciable interaction between the two metal centers within the limits of the electrochemical technique. On the other hand, the emission band characteristic of the Ru(II)-based unit is almost completely quenched with concomitant sensitization of the emission of the Os(II)-based unit. This observation demonstrates that electronic energy transfer takes place from the Ru(II)-based to the Os(II)-based unit. In particular, the  $^3\text{MLCT}$  state of the Ru(II)-based unit decays by two distinct processes with rate constants of  $2.0 \times 10^8$  and  $2.2 \times 10^7 \text{ s}^{-1}$

at 298 K, as observed by the biexponential decay of the Ru(II)-based phosphorescence intensity. This finding is likely related to the presence of two conformers. The steric hindrance between hydrogen atoms of pyridine and phenyl rings forces the Ru-based and Os-based subunits to assume two possible conformations: in the *cis* structure the two metal ions lie on the same side of the plane defined by the shape-persistent macrocycle **M**, whereas for the *trans* conformer the two metal ions lie on opposite sides. From space-filling models, the metal–metal distance is estimated to be ca. 1.5 nm for the *cis* conformer and ca. 1.7 nm for the *trans* conformer. These distances are lower than that estimated for the  $[\text{Ru}(\text{bpy})_3]^{2+}-(\text{ph})_3-[\text{Os}(\text{bpy})_3]^{2+}$  wires discussed above: if  $n = 3$ , the metal-metal distance is 2.4 nm and the rate constant is  $5.9 \times 10^{10} \text{ s}^{-1}$  at 298 K, ca. 300 times larger than the higher rate constant observed for the shape persistent macrocyclic bridge, demonstrating the importance of the bridge in mediating electronic interactions.

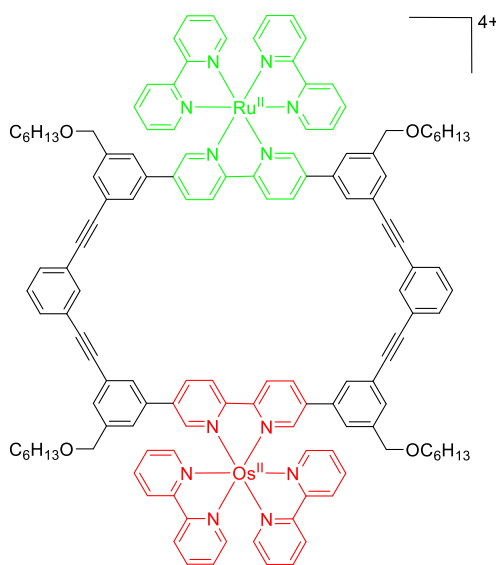


**Figure 13.** Structure of the complex  $[(\text{bpy})_2\text{Ru}(\mathbf{M})\text{Os}(\text{bpy})_2]^{4+}$  [25].

**Photoinduced electron transfer.** The  $[(\text{bpy})_2\text{Ru}^{\text{II}}(\mathbf{M})\text{Os}^{\text{III}}(\text{bpy})_2]^{5+}$  complex can be produced by quantitative oxidation of the Os(II)-based unit of  $[(\text{bpy})_2\text{Ru}(\mathbf{M})\text{Os}(\text{bpy})_2]^{4+}$  by Ce(IV) or nitric acid. The formation of the Os(III)-based unit is demonstrated by the appearance of an absorption band peaked at 720 nm ( $\epsilon_{\text{max}} = 250 \text{ M}^{-1}\text{cm}^{-1}$ ), attributed to a ligand-to-metal charge transfer band as confirmed by the study of the spectral changes observed upon oxidation of  $[(\text{bpy})_2\text{Os}^{\text{II}}(\mathbf{M})\text{Os}^{\text{II}}(\text{bpy})_2]^{4+}$ . Light

excitation of the Ru(II)-based unit of  $[(bpy)_2Ru^{II}(M)Os^{III}(bpy)_2]^{5+}$  is followed by electron transfer from the Ru(II)-based to the Os(III)-based unit ( $k_{el,f} = 1.6 \times 10^8$  and  $2.7 \times 10^7 \text{ s}^{-1}$ ). The so-formed transient  $[(bpy)_2Ru^{III}(M)Os^{II}(bpy)_2]^{5+}$  complex relaxes to the  $[(bpy)_2Ru^{II}(M)Os^{III}(bpy)_2]^{5+}$  species by back electron transfer ( $k_{el,b} = 9.1 \times 10^7$  and  $1.2 \times 10^7 \text{ s}^{-1}$ ). As previously discussed for energy transfer, the presence of two rate constants for the forward and backward electron-transfer processes can be rationalized on the basis of two conformers with *cis* and *trans* conformation of the Ru- and Os-based units. Comparison of the results obtained with those previously reported for other Ru-Os polypyridine complexes shows that the macrocyclic ligand **M** is a relatively poor conducting bridge.

### 2.3. Switching electron and energy transfer processes

Molecular bridging units whose energy or redox levels can be manipulated by an external stimulus can play the role of switches for the energy- or electron-transfer processes. In an appropriately designed compound, the external stimulus can be light. Since, by definition, switching has to be reversible, reversible photochemical reactions have to be used and photochromic molecules are particularly useful in this regard [3]. An example of molecular wire incorporating a switching unit is represented by a  $[Ru(bpy)_3]^{2+}$  and a  $[Os(bpy)_3]^{2+}$  moieties linked by an anthracene unit (Figure 14) [27, 28].

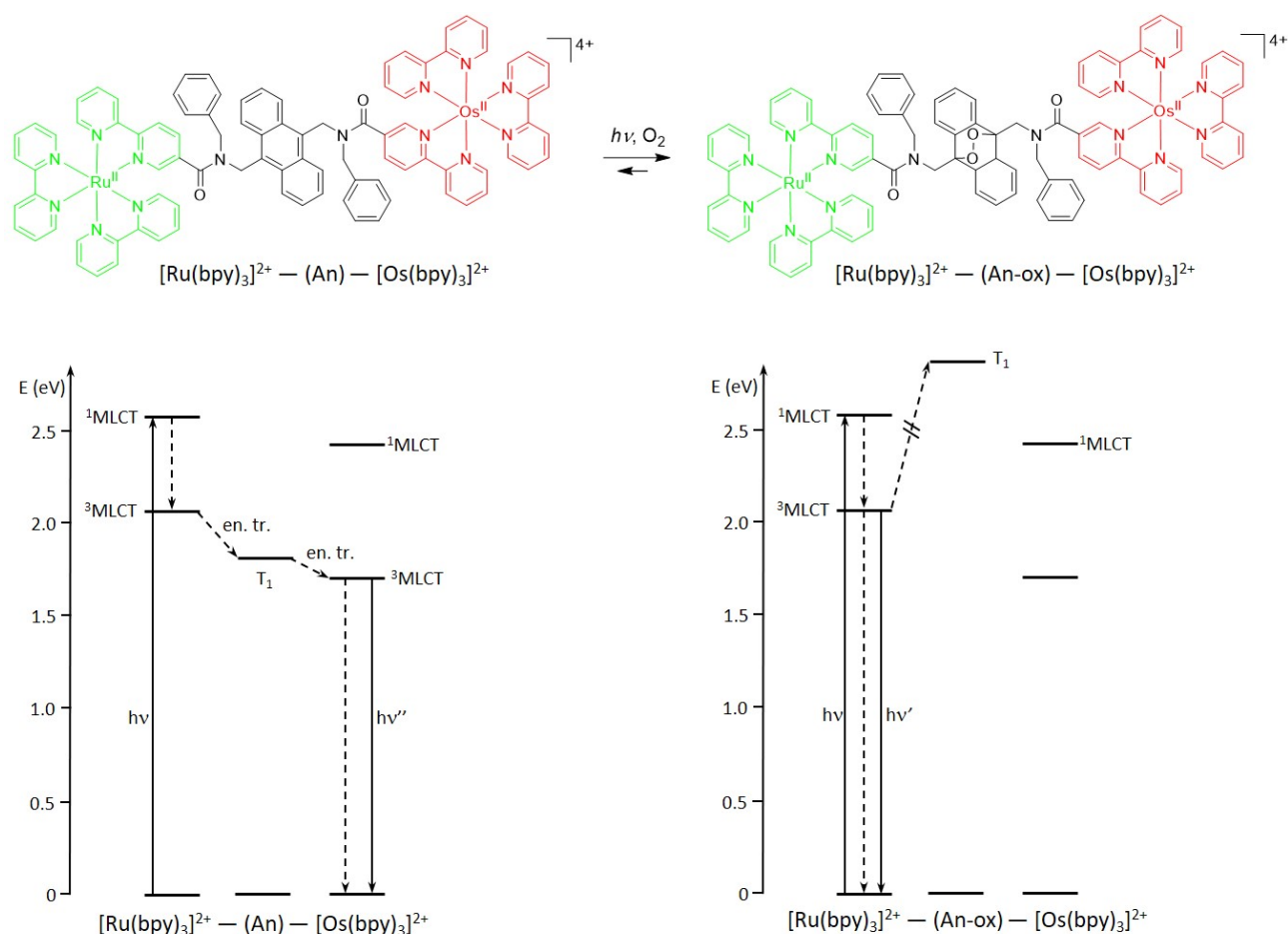


**Figure 14.** Molecular wire for energy transfer incorporating an anthracene switch [27, 28].

Upon selective excitation of the Ru(II)-based unit, sensitized emission of the Os(II)-based unit is observed (Figure 14,  $[\text{Ru}(\text{bpy})_3]^{2+}-(\text{An})-[\text{Os}(\text{bpy})_3]^{2+}$ ): a very efficient energy transfer occurs since the lowest triplet energy level of the anthracene bridge lies in between the lowest  $^3\text{MLCT}$  excited state of the Ru- and Os-based complexes. No change in the photophysical properties of the system is observed by continuous irradiation with visible light in deaerated acetonitrile solution. On the other hand, upon prolonged irradiation in aerated solution, the relatively long-lived  $^3\text{MLCT}$  of the  $[\text{Os}(\text{bpy})_3]^{2+}$  moiety sensitizes the population of singlet oxygen which reacts with the anthracene bridge to form the endoperoxide derivative (Figure 14,  $[\text{Ru}(\text{bpy})_3]^{2+}-(\text{An-ox})-[\text{Os}(\text{bpy})_3]^{2+}$ ). As a consequence, the delocalization of the  $\pi$ -system on the bridge is reduced, the lowest energy excited state of the bridge moves to much higher energy, and energy transfer is switched off. In principle, the process is reversible and the endoperoxide could be transformed back to anthracene, but such a reaction is difficult to perform.



## 2.4. Energy reservoir

As previously discussed, functionalization of the ligand by electron donating or electron accepting moieties affects the photophysical and redox properties of Ru(II) oligopyridine compounds, so that we can engineer, to some extent, the energy of the absorption and emission bands. On top of that, bridging Ru(II) complexes with other moieties in supramolecular systems promotes the occurrence of intramolecular quenching or sensitization processes: in both cases, the luminescent excited state lifetime cannot increase. Elongation of an excited state lifetime is a complex task, but highly desirable for a variety of applications, such as sensitized reactions, time-gated detection in sensing processes to shut off the background emission and autofluorescence of the sample. The so-called *energy reservoir* effect enables the lifetime prolongation in a supramolecular system.

The first example, reported in 1992 [29], was again based on a Ru(II) oligopyridine complex, whose lifetime was increased by more than one order of magnitude by linking the metal complex to a pyrene chromophore. This elongation is made possible by the occurrence of a reversible triplet-triplet energy transfer (Figure 15): the luminescent  $^3\text{MLCT}$  of the Ru(II) polypyridine complex is slightly higher than the lowest-lying, long-lived  $T_1$  of the pyrene chromophore and the energy difference between the two triplet states is sufficiently low to enable the thermal equilibration between these excited states at room temperature. Upon excitation of the Ru(II) complex, the  $^3\text{MLCT}$ , populated by a highly efficient inter system crossing, undergoes energy transfer to the lower lying  $^3(\pi,\pi^*)$  state of the pyrene, followed by a back energy transfer  $^3(\pi,\pi^*) \rightarrow ^3\text{MLCT}$ . The lifetime elongation is based on the temporary storage of the excitation energy (*energy reservoir*) on the long-lived  $T_1$  state of the pyrene chromophore. Eventually, the  $^3\text{MLCT}$  state of the Ru(II) complex undergoes delayed deactivation. The Ru(II) complex and pyrene chromophore assume a common deactivation rate constant which is a combination of the rates of the two individual moieties. The net effect is the emission of the Ru(II) complex with the emission quantum yield typical of the pristine compound, and an increased lifetime.

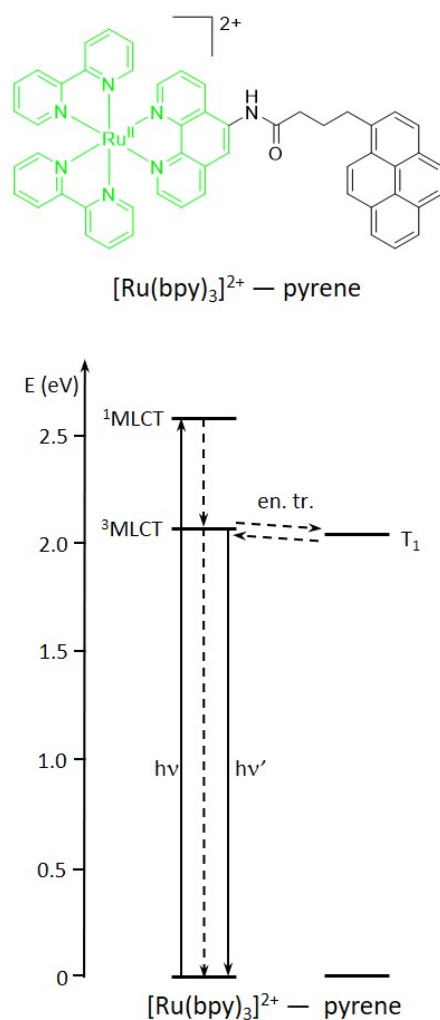


**Figure 15.** Energy level diagram for energy reservoir in  $[\text{Ru}(\text{bpy})_3]^{2+}$  - pyrene [29].

The efficiency of this process depends on different factors, among which: (i) the efficiency of the inter system crossing of the metal complex, (ii) the energy difference between the two equilibrated excited states, (iii) the temperature, and (iv) the lifetimes of the involved excited states. The rate of the thermal back energy transfer must be significantly faster than the intrinsic deactivation of the lower-lying triplet excited state (pyrene-based in this example). This process is temperature dependent and it can be shut off at 77 K.

A powerful strategy to extend further the excited state lifetime of a given chromophore relies on appending several reservoir units, thus increasing the efficiency of the energy-transfer process, taking advantage of statistical effects [30].

The same strategy was employed to extend the lifetime of the  $[\text{Ru}(\text{tpy})_2]^{2+}$  complex, which is much shorter lived than the prototypical  $[\text{Ru}(\text{bpy})_3]^{2+}$  because of the non-radiative deactivation to the  $^3\text{MC}$  excited state.

The Ru(II) metal ions is complexed by 2,2':6',2''-terpyridine (tpy) ligands connected to a terthiophene unit via an alkynyl bridge (Figure 16) [31]. The absorption spectrum is not the mere sum of the terthiophene and  $[\text{Ru}(\text{tpy})_2]^{2+}$  chromophores: the tpy and terthiophene absorption bands are strongly overlapped and red-shifted because of the strong conjugation between the two moieties owing to the alkynyl bridge and the characteristic MLCT transition in the visible spectral region is bathochromically shifted and with a larger molar absorption coefficient compared to pristine  $[\text{Ru}(\text{tpy})_2]^{2+}$ . The larger oscillator strength of the MLCT transition is caused by the extension of the  $\pi$ -conjugated system on the terpyridine ligand that induces a larger dipolar moment for the MLCT transition [32]. A phosphorescence is observed at room temperature with red-shifted band maximum ( $\lambda_{\text{em}} = 698 \text{ nm}$ ) and a significantly longer excited state lifetime ( $\tau = 435 \text{ ns}$ ) compared to the pristine  $[\text{Ru}(\text{tpy})_2]^{2+}$  complex ( $\lambda_{\text{em}} = 629 \text{ nm}$ ,  $\tau = 0.25 \text{ ns}$ ). Indeed, the luminescent  $^3\text{MLCT}$  state lies very close in energy to the long-lived  $T_1$  excited state of terthiophene ( $\tau = 62 \mu\text{s}$  in degassed acetonitrile solution at 298 K), so that reversible energy transfer can take place by equilibration of these close-lying excited states. Further confirmation of this mechanism comes from transient absorption spectroscopy. Upon 532 nm-laser excitation of an acetonitrile degassed solution of the complex, an absorption band with maximum at 435 nm, typical of the  $T_1$  excited state of terthiophene, is observed and the corresponding lifetime is the same (435 ns) as that measured by phosphorescence intensity decay of  $^3\text{MLCT}$ . This result demonstrates a common decay rate of the two equilibrated triplet excited states. The lifetime of the  $^3\text{MLCT}$  state the Ru(II) unit increased by more than 3 orders of magnitude: from 0.25 to 435 ns at 298 K. This strong increase is likely due to the very close lying triplet excited state of the Ru(II) complex and the terthiophene unit and the strong  $\pi$ -conjugation enabled by the alkynyl bridge.

The energy reservoir effect is recently attracting increasing interest [33, 34] in a variety of fields from oxygen sensing [35], conformational probe [36] to energy up-conversion [37].

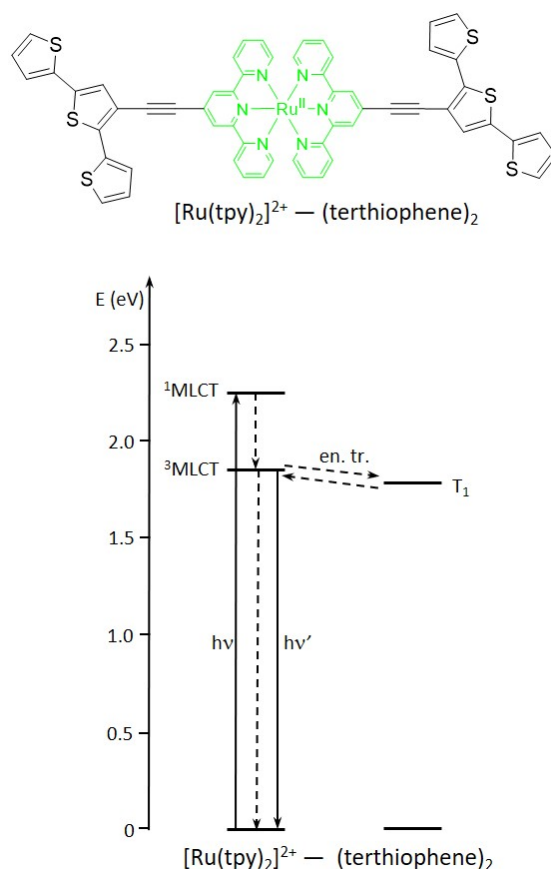


**Figure 16.** Energy level diagram for the system  $[\text{Ru}(\text{tpy})_2]^{2+} - (\text{terthiophene})_2$  exhibiting energy reservoir [31].

### 3. Dendrimers

Dendrimers are a class of multibranched molecules exhibiting a defined structure and a high degree of order and complexity [38]; from a topological viewpoint, three different regions can be distinguished in their structure: core, branches, and periphery. Furthermore, the branches can be constituted by successive layers of concentric shells the number of which defines the dendrimer generation (Figure 17).

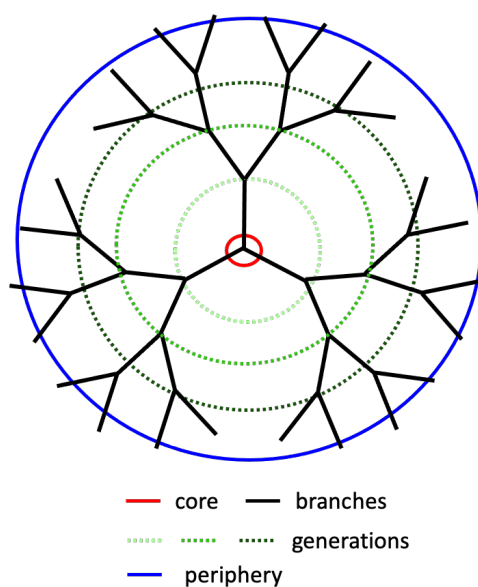


**Figure 17.** Schematic representation of a dendrimer.

By using suitable synthetic strategies [38], it is possible to place selected functional groups in one, or two, or all of these regions of the dendritic architecture; therefore a variety of dendrimers can be obtained depending on the number and nature of the incorporated functional groups and the degree of functionalization. Moreover, the presence of internal dynamic cavities in the three-dimensional structure enables dendrimers to non-covalently link ions or molecules [39].

As a consequence of these features, dendrimers may exhibit remarkable physical, chemical, and biological properties and have potential applications in different fields such as physics, chemistry, biology, medicine and engineering [40]. For example, dendrimers incorporating luminescent units [41] and/or behaving as ligands of metal ions [41a, 42] can lead to interesting photophysical properties [43], and have a variety of applications, including (i) sensing with signal amplification [41d, 44], (ii) quenching and sensitization processes [45], and (iii) light harvesting [46]. On the other hand, dendrimers containing redox-active groups can find useful applications as sensors [44, 47], catalysts [44, 47, 48], and enzyme mimics [49], in which an electro-active centre is buried inside the dendrimer environment. Furthermore, dendrimers capable of exchanging several electrons at the same potential can perform the function of charge storage devices [44, 47, 50, 51] with interesting potential applications; for example they can be exploited as catalysts for multielectron processes and molecular batteries to power in the future molecular machines or to construct flexible rechargeable batteries [52].

It is also important to notice that the presence of redox-active groups is useful to gain important information from a fundamental viewpoint; indeed, electrochemistry is a powerful technique (i) to elucidate the structure and superstructure of the dendrimer (therefore, also its purity), (ii) to evaluate the degree of electronic interaction and communication among the redox units located in different sites of the dendritic architecture; and (iii) to investigate the changes in conformation caused by electron-transfer processes.

$[\text{Ru}(\text{bpy})_3]^{2+}$ -type complexes, but also Ru-polypyridine complexes in general, because of their already seen peculiar photochemical and electrochemical properties, are functional components particularly suitable to obtain photo- and electro-active dendrimers exhibiting remarkable features, as shown by the following selected examples investigated in our laboratory.

### 3.1. Dendrimers with a $[\text{Ru}(\text{bpy})_3]^{2+}$ -type complex in the core

By exploiting the fact that 2,2'-bipyridine can be easily functionalised in the 4 and 4' positions, dendrimers containing a  $[\text{Ru}(\text{bpy})_3]^{2+}$ -type unit as a core surrounded by branches of different chemical composition and increasing dimension can be prepared.

Dendrimer **1** (Figure 18) is made of a Ru-complex core surrounded by branches containing dioxybenzene- and oxybenzene-type groups that are redox-active and potentially luminescent [53]. From the electrochemical point of view, several processes are therefore expected: reduction concerning the bpy-type ligand and oxidation involving the metal-complex moiety and the aromatic units of the branches. Accordingly, cyclic (CV) and differential pulse (DVP) voltammetric patterns are quite complex, particularly on the oxidation side because of the presence of several and overlapping processes. It was, however, possible to estimate the potential value for the Ru(III)/Ru(II) process and to evidence that in such a process less than one electron is exchanged. Comparison with the data obtained for the  $[\text{Ru}(\text{Me}_2\text{bpy})_3]^{2+}$  model compound shows that in **1** the oxidation and reduction processes of the core take place at more positive potential values and that they are not fully kinetically reversible, a behavior that is typical of encapsulated units.

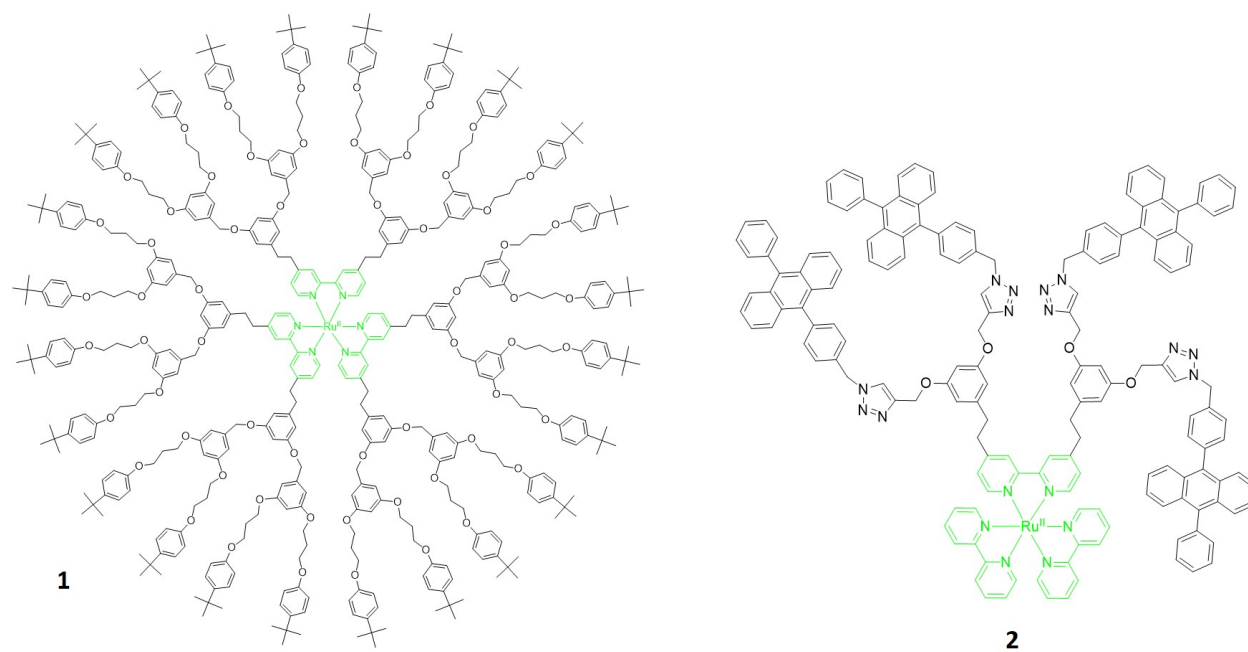


**Figure 18.** Structural formulas of dendrimers **1** [53] and **2** [58].

As far the spectroscopic investigations are concerned, it is interesting to note that, although all the units present in the dendrimer absorb light and are potentially luminescent, only the characteristic emission of the  $[\text{Ru}(\text{bpy})_3]^{2+}$ -type is observed. Such a result shows that an efficient energy transfer from the aromatic units of the branches to the core occurs with the concomitant sensitization of the orange luminescence of the Ru-complex, regardless of the excitation wavelength. Therefore, this dendrimer, in which many chromophoric units absorb the incident light and then channel the excitation energy to a common acceptor component, behaves as an antenna for light harvesting [54, 55].

The effect of the branches in encapsulating the core, already observed in the electrochemical experiments, is also evidenced by the fact that in **1** the Ru-based luminescence is quenched by dioxygen less efficiently than in the case of the  $[\text{Ru}(\text{Me}_2\text{bpy})_3]^{2+}$  model compound.

The luminescence features of dendrimer **1** have been improved [56] by replacing the 4'-*tert*-butylphenoxy peripheral units with naphthyl moieties that exhibit a strong absorption and a very short-lived fluorescence in the UV spectral region. As for **1**, also in the case of this dendrimer the emission of the units incorporated in the branches is almost completely quenched with the concomitant sensitization of the orange Ru-based luminescence, via a very efficient energy transfer from the branches to the core. With respect to **1** the improvement consists in the fact that, because of

the high absorbance of the naphthyl moieties, the very efficient energy-transfer process, and the strong emission of the core, this dendrimer shows a noticeable visible emission upon UV excitation even in diluted solution, up to  $10^{-7}$  mol L<sup>-1</sup>. Therefore, this dendrimer is an antenna for light harvesting more efficient than dendrimer **1**.

Dendrimers can be exploited not only to obtain light-harvesting antennae in which the photons emitted are at energy lower than that of the absorbed ones, as in the case of the two dendrimers just described; if suitably designed, dendrimers can be also used to get energy up-conversion, the process in which incident photons of a given energy are converted into photons of higher energy [37, 57]. An example of such behavior is given by dendrimer **2** (Figure 18) made of a [Ru(bpy)<sub>3</sub>]<sup>2+</sup>-type core and four diphenylanthracene units at the periphery [58]. The photophysical experiments show the occurrence of a complex pattern of energy- and electron-transfer processes; in particular they clearly evidence that, upon green-laser light excitation at 532 nm of the Ru-complex core, the blue emission of the diphenylanthracene chromophores appears both in fluid solution and in rigid matrix at 77 K. The novelty of this study is the use of a multichromophoric system in which energy and electron transfers are intramolecular processes and in which, therefore, energy up-conversion works even in solid state.

### **3.2. Dendrimers with Ru polypyridine-type complexes at their periphery**

Dendrimers incorporating in their structure multiple, chemically identical, and non-interacting redox-active units are capable of exchanging several electrons at the same potential value. If the component units undergo chemical reversible and fast electron-transfer processes and exhibit chemical robustness under the working conditions, dendrimers of this kind perform as charge-storing devices [59, 60] that are important for their potential, already mentioned applications.

Poly(amido-amine) (PAMAM) dendrimers decorated at the periphery with Ru polypyridine-type complexes are good candidates as charge-storing devices thanks to the peculiar redox properties of the Ru complexes. Therefore, they have been extensively investigated from the electrochemical viewpoint [61]. In this regard, the most interesting electron-transfer process is the first metal-centered oxidation process, and the first ligand-centered reduction. Furthermore, in all the reported examples a single cyclic voltammetric wave is observed, on the reduction and oxidation sides, evidencing the



electrochemical equivalency of all the peripheral redox units, an important requirement to behave as multielectron storage devices.

The largest investigated dendrimer of this kind is the fourth generation PAMAM dendrimer decorated at the periphery with 64  $[\text{Ru}(\text{bpy})_3]^{2+}$ -type, or  $[\text{Ru}(\text{tpy})_2]^{2+}$ -type complexes (dendrimers **3** and **4**, respectively, of Figure 19a) [61a,d].

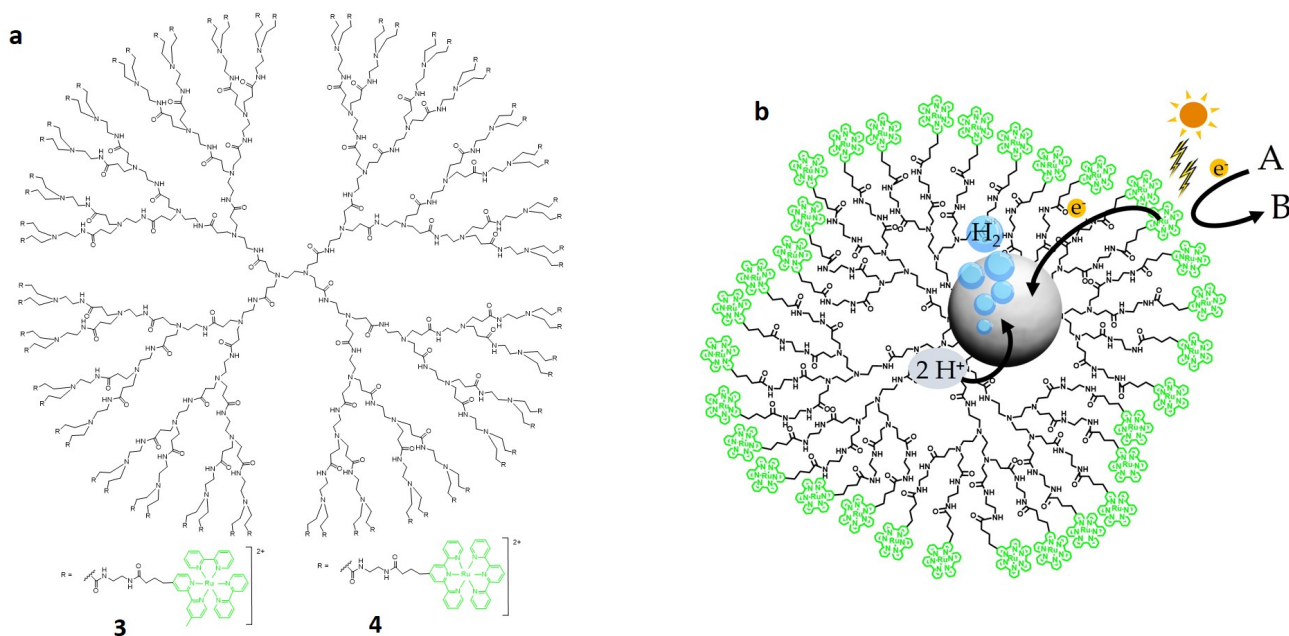


**Figure 19.** (a) Structural formulae of the fourth generation PAMAM dendrimers **3** and **4** [61]. (b) The third generation PAMAM dendrimer decorated at the periphery with 32  $[\text{Ru}(\text{bpy})_3]^{2+}$ -type complexes is used as scaffold to combine the sensitizer and the catalyst for the water photoreduction [62].

As expected, they show a metal-based oxidation process and two reduction processes that are attributed to the first and second reduction of the polypyridine ligands. A more detailed electrochemical investigation by using ultrafast voltammetry has been carried out on dendrimer **4** adsorbed on a Pt disk ultramicroelectrode [61b,c]; from the obtained data it was possible not only to measure the rate of the self-exchange electron transfer for the peripheral  $[\text{Ru}(\text{tpy})_2]^{2+}$ -type complexes, but also to establish that the dendrimer adsorbed on the electrode surface does not keep its “usual” globular form, but assumes a hemispherical shape.

The third generation PAMAM dendrimer decorated at the periphery with 32  $[\text{Ru}(\text{bpy})_3]^{2+}$ -type complexes was studied in aqueous solution [62] evidencing that the dendrimer absorption spectrum exhibits the LC band in the UV region and the MLCT band in the visible region typical of the  $[\text{Ru}(\text{bpy})_3]^{2+}$  complex; also the emission band is identical in shape and energy to that of the  $[\text{Ru}(\text{bpy})_3]^{2+}$ , although the emission quantum yield is half, probably because of an electron-transfer process involving the amine moieties of the dendritic branches.

The Ru-based emission was then used to investigate the capability of the dendrimer to coordinate  $\text{Pt}^{2+}$  ions and, after their reduction with  $\text{NaBH}_4$ , to host in its cavity Pt nanoparticles; it is, indeed, well known that PAMAM structures can behave as templates of metal nanoparticles [63]. The results obtained have evidenced that each dendrimer can coordinate 20 equivalents of  $\text{Pt}^{2+}$  and that 40% of them are reduced giving nanoparticles with an average diameter of  $1.3 \pm 0.3$  nm and an average atom number of 76. It is interesting to notice that this latter data suggests the cooperation of at least three different dendrimers for the nanoparticle formation.

The system so prepared is, therefore, a dendrimer containing inside its cavities Pt nanoparticles and incorporating at its periphery the  $[\text{Ru}(\text{bpy})_3]^{2+}$ -type complexes that are capable to absorb visible light and behave as photosensitizers; because of these features and taking inspiration from the seminal paper of Balzani et al. [64], the system was exploited to induce the photoreduction of water using ascorbic acid as sacrificial electron donor (Figure 19b). Photo-evolution of  $\text{H}_2$  was, in fact, observed with the maximum rate of  $67.2 \text{ nmol h}^{-1}$  that corresponds to a turnover frequency of  $44.5 \text{ h}^{-1}$  per Pt nanoparticle, a result in line with those reported for supramolecular systems involving a Ru(II) polypyridine dye and a molecular catalyst [65]. However, in comparison to the previous investigations, this study has an important novelty that consists in the use of a dendrimer suitably prepared to perform simultaneously three different tasks: ligand for  $\text{Pt}^{2+}$  ions, template for the formation of the nanoparticles and stabilizer to prevent their aggregation, and, finally, photosensitizer for the reduction of water thanks to the chromophoric units present in its periphery.

### 3.3. Dendrimers with Ru polypyridine-type complexes as the branching elements

In the past twenty years a great number of studies have been carried out on Ru-polypyridine complexes; their photophysical and redox properties have been investigated and the use of model

design has enabled to fine tune their spectroscopic and electrochemical features [6, 9]. This library of compounds was the starting point to design polynuclear metal dendrimers in which the Ru complexes occupy each site of the dendritic structure.

The very efficient synthetic strategy called “complexes as ligands/complexes as metals” [66], together with the use of suitable bridging, 2,3- and 2,5-bis(2-pyridyl)pyrazine (2,3- and 2,5-dpp), and terminal, bpy and 2,2'-biquinoline (biq), ligands, enabled to prepare dendrimers containing 4, 6, 10, 13, and 22 Ru(II) metals and exhibiting an interesting behavior from the photophysical and electrochemical points of view [50, 67]. As far as the spectroscopic investigations are concerned, the obtained results can be interpreted on the basis of the following considerations. First, such dendrimers can be viewed as an ordered assembly of  $[\text{Ru}(\text{L})_n(\text{BL})_{3-n}]^{2+}$  mononuclear units (L = bpy or biq; BL = 2,3- or 2,5-dpp) with specific photophysical properties. Second, the relatively small, but not negligible electronic interaction between nearby units does not influence the absorption feature, whereas is sufficient to lead very fast energy-transfer processes; these processes cause the quenching of the potentially luminescent units with higher  $^3\text{MLCT}$  levels and lead to the luminescence sensitization of the units with lower  $^3\text{MLCT}$  levels.

Because the energy of the  $^3\text{MLCT}$  excited state for each unit depends on the nature of the coordinated ligands and on its position in the dendritic structure, the efficient synthetic strategy used leads to a high degree of energy-transfer control. An example is the docosanuclear dendrimer [68] shown in Figure 20, that contains 22 Ru centers, 24 terminal bpy ligands and 21 bridging 2,3-dpp ligands. It exhibits a huge absorption on the entire UV-Vis spectral region that is practically the sum of the spectra of the 22 constituent units, whereas its emission arises only from the 12 peripheral units evidencing that the energy absorbed by all the component units is very fast transferred to the peripheral ones, as expected because such units have their  $^3\text{MLCT}$  levels at lowest energy.

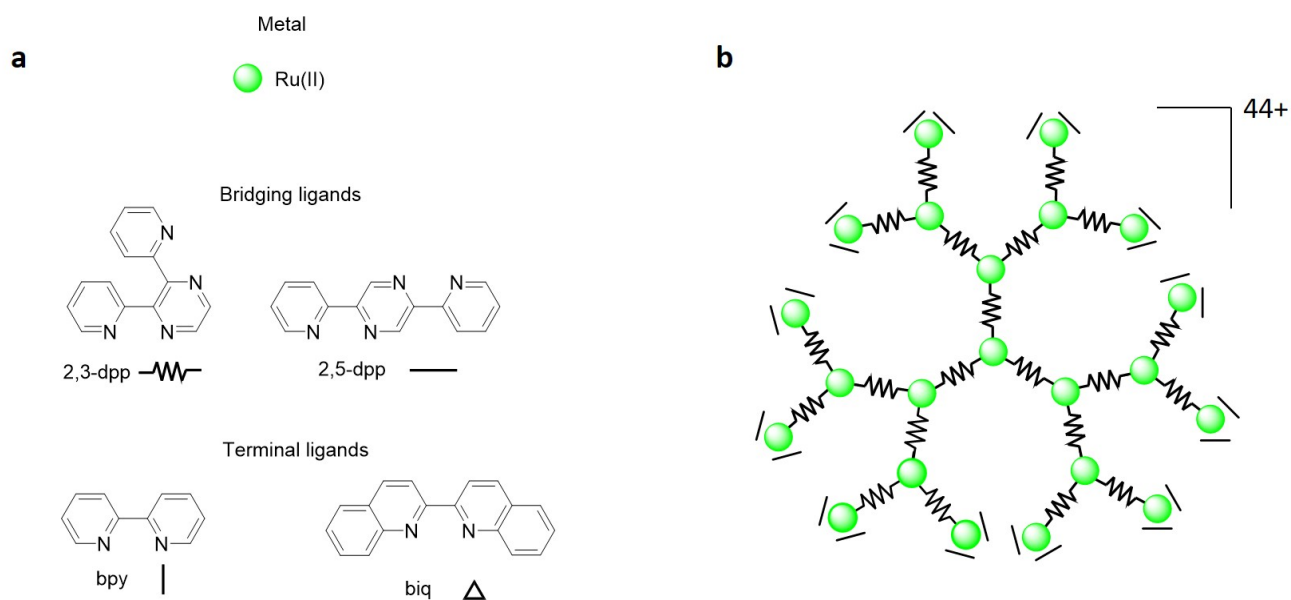


**Figure 20.** (a) Structural formulae, abbreviations and graphic symbols used to represent the components of the Ru-based polynuclear dendrimers. (b) Schematic representation of the docosanuclear dendrimer containing 22 Ru centers [68].

Concerning the electrochemical investigation, the obtained results can be rationalized once again viewing the dendrimers as made of mononuclear units that have their own redox properties. Accordingly, each unit shows, on oxidation, one metal-based process occurring at a potential value that depends on the nature of the coordinated ligands; in particular, the potential is shifted to less positive values on increasing the ligand electron-donor power that changes in the order  $\mu\text{-2,5-dpp} < \mu\text{-2,3-dpp} < \text{biq} < \text{bpy}$ . On the reduction side, the processes are ligand localized: each terminal ligand is reduced twice and each bridging ligand, when it is coordinated to a metal ion, is reduced four times [69]; the potential values at which such processes occur depend, of course, on the nature of the ligand, but also on the nature of the other ligands coordinated to the metal.

The mononuclear units bring their redox properties in the dendritic structure, although they can be affected by intercomponent interactions: interactions between metal-metal and ligand-ligand are noticeable if the metals are coordinated to the same bridging ligand and if the ligands are coordinated to the same metal, whereas the interactions are practically negligible in the case of metals and ligands that are sufficiently far apart. Because the high degree of the synthetic control enables to place selected units in the desired sites of the structure, dendrimers with predetermined redox patterns can be

obtained; in particular, the number's control of chemically equivalent and non-interacting units translates in the control of the electrons lost or gained at a certain potential value and, therefore, in the possibility to exploit such dendrimers as charge-storing devices. For example, in the docosanuclear dendrimer previously mentioned [68] oxidation involves the peripheral units that are equivalent, as evidenced by the presence of a twelve-electron oxidation wave at 1.52 V vs SCE; the oxidation processes involving the other component units are shifted to higher potential values and cannot be observed in the potential window accessible for the used acetonitrile solvent [70]. On the reduction side, many overlapping and hardly assigned waves are present, as expected because of the involvement of several terminal and bridging ligands, each capable of undergoing multiple reductions. Such a complex reduction behavior, however, should not be considered a negative aspect for potential applications of these polynuclear dendrimers.

For example, very good results for oxygen production (60% of the absorbed photons are used to produce O<sub>2</sub>) in photoinduced water oxidation experiments have been obtained using, together with a molecular tetra-ruthenium polyoxometalated species as catalyst and persulfate anions as sacrificial acceptor, a tetranuclear dendrimer of this family that plays the photosensitizer role [71]. As clearly demonstrated, the excellent performance of the system has to be attributed to the use of the dendrimer for two main reasons. The first one concerns the spectroscopic properties of the dendrimer, whose absorption spectrum overlaps the solar emission spectrum much better than [Ru(bpy)<sub>3</sub>]<sup>2+</sup>, the most commonly used photosensitizer. The second and more important reason is ascribed to the fact that the positively charged dendrimer and the negatively charged polyoxometalated catalyst are strongly ion-paired in solution, and larger aggregates are also formed, favoring the occurrence of the needed electron-transfer processes.

A final consideration concerns the effective structure of these metal-based dendrimers that is still an open question. In fact, each Ru unit can exist in two chiral forms and, moreover, it can have a *fac* or *mer* conformation; therefore, in principle the number of isomers is very high, in particular on increasing dendrimer nuclearity. However, it has been demonstrated that the photophysical and electrochemical properties of these compounds are independent of chirality and geometrical arrangement of their component units.

**Extension to other metals and other ligands.** The good spectroscopic and electrochemical features of these Ru-based dendrimers can be further improved by inserting in the structure component units with

metals and/or ligands different from those described above, like Os(II) polypyridine complexes, or Rh(III) and Ir(III) cyclometalated complexes. In such a way gradients for photoinduced directional energy and electron transfer, as well as sites for multielectron exchange, can be better controlled [50, 68].

For space reasons only six decanuclear dendrimers containing Ru(II) and Os(II) ions are very briefly described in the following. As shown in Figure 21, they contain a different number of Ru(II) and Os(II) ions, suitably distributed in the dendritic structure and linked by the 2,3-dpp bridging ligands, and carry at their periphery bpy or biq terminal ligands [72].

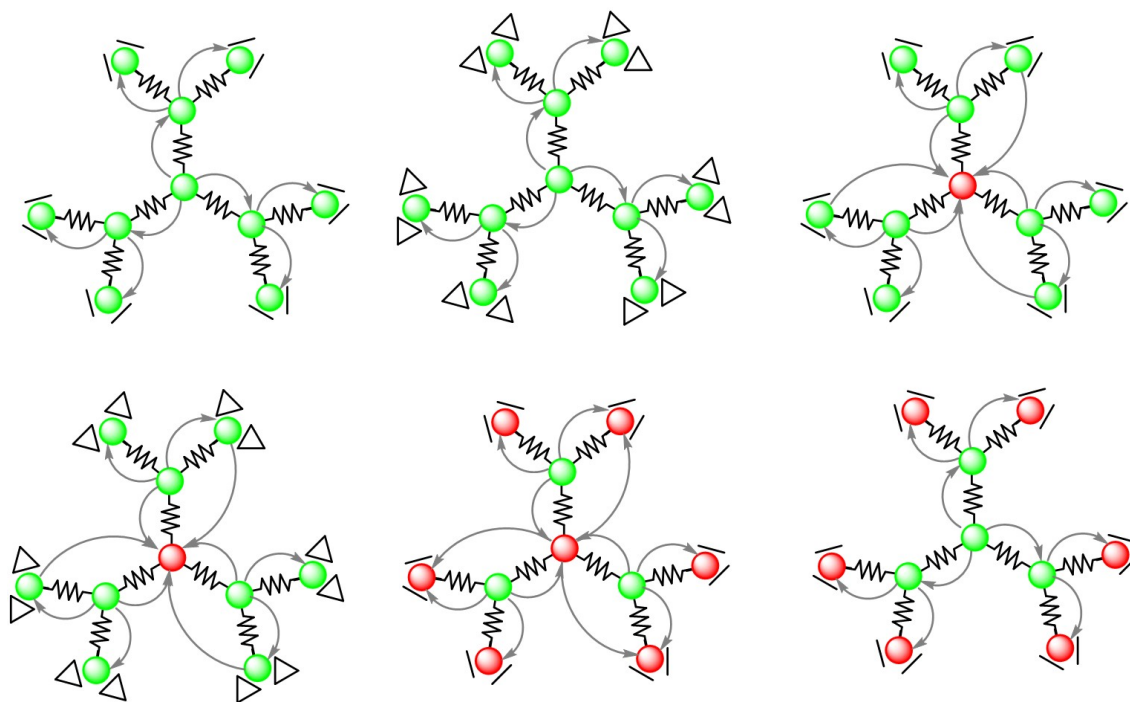


**Figure 21.** Schematic representation of six decanuclear dendrimers containing a different number of Ru(II) and Os(II) (green and red circles, respectively); the graphic symbols used to represent the ligands are those displayed in Figure 20a. The arrows indicate the energy-transfer patterns that can be obtained in such dendrimers [72].

From the spectroscopic point of view, the absorption bands with very large molar absorption coefficients in the UV (LC bands) and visible (MLCT bands) spectral region are ascribed to the component units. The luminescent properties of these dendrimers show that energy-transfer processes

occur (Figure 21) within the dendritic array, from the center to the periphery or *vice versa*. These results can be interpreted on the basis of the chemical nature of metals and terminal ligands and the structural location of metal centers, showing that the excitation energy can be channeled in the desired direction by a suitable choice of the components and of their location. It has to be noticed, however, that on increasing nuclearity, it is impossible to have an unidirectional gradient for energy transfer using only two types of metals and ligands [50].

The examined decanuclear dendrimers show also interesting electrochemical properties [72]; in particular it has been evidenced that the oxidation of the 10 metal ions depends not only on the nature of the metal ion, but also on its location in the dendritic array, as clearly shown by the redox patterns of three dendrimers of this family reported in Figure 22. Therefore, the electrochemical data offer a fingerprint of the chemical and topological structure of such compounds.

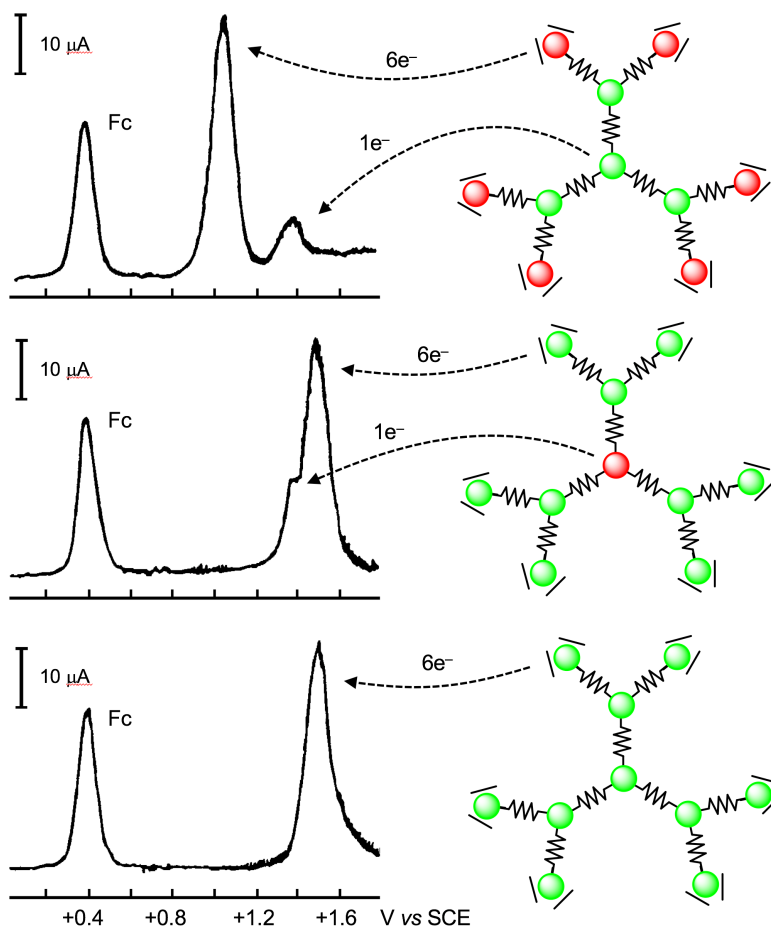


**Figure 22.** Redox patterns (DPV peaks) for three decanuclear dendrimers showing the selective oxidation of the different metals present in the structure (the graphic symbols used are those displayed

in Figures 20a and 21). Fc peak corresponds to the oxidation of ferrocene used as an internal standard. Adapted from ref. 72.

### 3.4. A proton-driven assembly of a luminescent dendrimer with a Ru bpy-type complex

Suitably designed dendrimers and metal complexes can assemble to give supramolecular systems in which the dendrimer occupies the second coordination sphere.

An interesting example of this type of assembly (Figure 23) involves the  $[\text{Ru}(\text{bpy})(\text{CN})_4]^{2-}$  complex and a dendrimer consisting of a 1,4,8,11-tetraazacyclotetradecane (cyclam) core appended with 12 dimethoxybenzene and 16 naphthyl moieties [73].

A 1:1 mixture of the two components exhibits the absorption and emission bands characteristic of the isolated compounds, evidencing that there is no interaction between them.

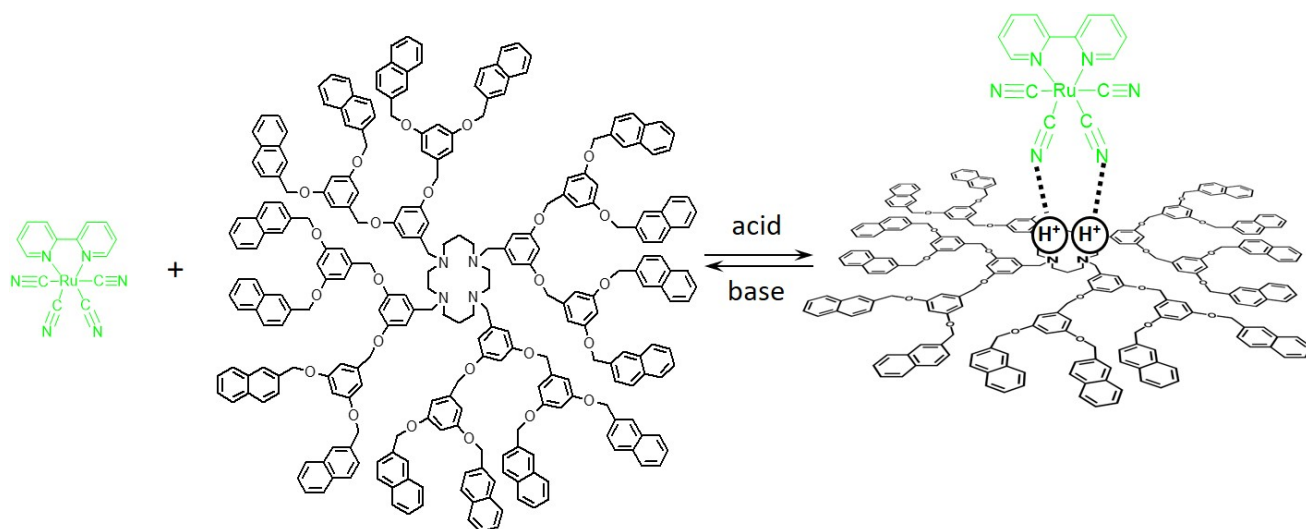


**Figure 23.** The proton-driven formation of the adduct involving a cyclam-based dendrimer and the  $[\text{Ru}(\text{bpy})(\text{CN})_4]^{2-}$  complex [73].

However, acid addition causes strong spectral changes; the obtained results show that, when two equivalents of acid are added, the adduct reported in Figure 23 is formed, in which the two starting species share two protons. In the adduct the fluorescence of the dendrimer naphthyl moieties is strongly quenched by very efficient energy transfer to the Ru complex, as evidenced by the sensitization



of its luminescence. According to this finding, the dendrimer plays the role of a light-harvesting second coordination sphere that channels the collected energy to the  $[\text{Ru}(\text{bpy})(\text{CN})_4]^{2-}$  complex.

The adduct can be subsequently disrupted by the addition of a base with restoration of the starting species.

Therefore, in this supramolecular system, by modulating the interactions that keep the components together, it is possible to switch on/off the energy-transfer process.

Interestingly, such a system can be used as a logic gate; indeed, the adduct between the dendrimer and the complex, upon stimulation with two chemical (acid and base) inputs, exhibits two distinct optical (naphthyl-based and Ru-based emissions) outputs that behave, respectively, according to an XOR and an XNOR logic [73].

## **4. Molecular machines**

### **4.1. Basic concepts**

A molecular machine is a molecule, or an assembly of a defined number of molecular components, designed to perform large-amplitude and controlled movements of some of its parts relatively to others, in response to external stimuli [74]. The importance of biomolecular machines for living organisms is nowadays well established [75], and the development of artificial counterparts [76] is a flourishing research field [77, 78, 79, 80] that has been recently recognized by the award of the Nobel Prize in Chemistry to three of its pioneers [81, 82, 83]. The increasing experimental evidence of the potential utility of molecular machines in materials science and engineering, catalysis, medicine and information processing constitutes an important driver for real world applications [84, 85].

Among the different forms of energy that can be supplied to molecular machines, light is, for several reasons, a convenient choice to make them work [86]. An important advantage is that photons not only carry the energy to feed the machine, but can also be utilized to monitor its operation through spectroscopic methods. Indeed, the realization of synthetic molecular machines and motors that can harness sunlight energy to perform technologically relevant tasks (including the conversion and storage of the energy itself) is an exciting goal of nanotechnology.

The valuable, highly tuneable and, for certain aspects, unique photophysical, photochemical and redox properties of  $[\text{Ru}(\text{bpy})_3]^{2+}$  and related Ru(II) polypyridine complexes makes them ideal components to introduce light-induced functionalities in molecular machines [87]. This goal can be achieved either by an intermolecular or an intramolecular approach. In the former case, a ruthenium complex not chemically bound to the molecular machine becomes involved in a bimolecular encounter with a machine component in solution. In the latter case, a Ru-based moiety is covalently or mechanically linked to a machine component, according to a specific modular design.

In the following we will describe a few significant examples of artificial molecular machines containing Ru-polypyridine complexes as photosensitizers, categorized for the type of light-induced process and the kind of molecular architecture.

#### 4.2. Photoinduced energy transfer

**Rotary motors.** A very successful design for molecular machines is based on overcrowded alkenes (Figure 24). It is well known that compounds of this kind, whose archetype is shown in Figure 24a, can undergo light-driven repetitive and unidirectional rotation about the C=C double bond according to a cyclic sequence consisting of alternated *cis/trans* photoisomerization and thermal helix inversion steps, with the latter determining directionality [81]. In the attempt to shift the irradiation wavelength necessary to activate the motor from the near UV to the visible range, the stator portion of a second-generation motor was replaced with a 4,5-diazafluorenyl chelating unit [88]. Complexation to a  $[\text{Ru}(\text{bpy})_2]^{2+}$  moiety afforded a molecular motor wherein the stator subcomponent acts as a ligand for the Ru(II) ion (Figure 24b). Excitation with light of 450 nm, absorbed exclusively by the Ru polypyridine unit, was found to activate unidirectional rotation; at the same time, a quenching of the MLCT emission was observed. These results were interpreted in terms of energy transfer to the overcrowded alkene moiety, although no further data supporting this mechanism were collected. Another interesting observation was a large increase in the rotation rate for the Ru-complexed motor – a fact that was shown by DFT calculations to be a consequence of slight conformational changes of the diazafluorenyl portion as a result of coordination to the metal, thereby decreasing the steric hindrance between the stator and the rotor.

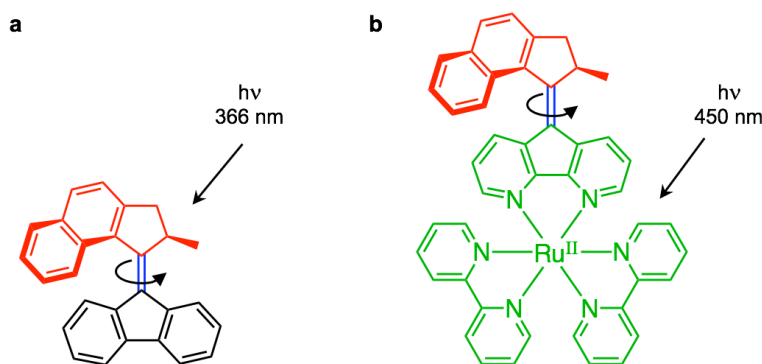


**Figure 24.** A second-generation overcrowded alkene rotary motor (a), driven by near-UV light, was modified in its lower half such that the new compound could function as a bidentate chelate ligand in a ruthenium complex (b). Irradiation in the Ru-based MLCT band at 450 nm triggers the unidirectional rotation about the double bond [88].

### 4.3. Photoinduced electron transfer

**Pseudorotaxanes.** These supramolecular complexes, consisting at minimum of a molecular axle threaded into a macrocycle, are relevant for molecular machines because external stimuli can be used to control the threading/dethreading of the components. Indeed, the first examples of artificial light-driven molecular machines took advantage of the dynamic features of pseudorotaxanes combined with the photosensitizing properties of  $[\text{Ru}(\text{bpy})_3]^{2+}$ -type complexes [89, 90, 91].

More recently, the efficiency of the photoinduced dethreading of a pseudorotaxane was enhanced when a bichromophoric system consisting of a  $[\text{Ru}(\text{bpy})_3]^{2+}$ -type complex and an appended pyrene unit, which exhibits the energy reservoir effect (Section 2.4), was used instead of plain  $[\text{Ru}(\text{bpy})_3]^{2+}$  [92]. The pseudorotaxane components are the well-known tetracationic cyclophane cyclobis(paraquat-*p*-phenylene) (CBPQT) and a naphthalene-based molecular axle (Figure 25). Their dethreading can be obtained by reduction of the bipyridinium units of CBPQT, a process that weakens the intercomponent charge-transfer (CT) interactions responsible for the complex stability. Such a reduction can be caused by light with the aid of a photosensitizer characterized by an excited state with enough reducing power and a sufficiently long lifetime. For the reasons explained in the previous Sections,  $[\text{Ru}(\text{bpy})_3]^{2+}$  is an ideal candidate for this role. To prevent the back electron transfer from the reduced macrocycle to the oxidized metal complex (which is faster than dethreading), an appropriate quantity of a sacrificial reductant needs to be added, so that the oxidized form of the photosensitizer is scavenged and its

original form is regenerated [89]. The  $^3\text{MLCT}$  excited state of the Ru complex shown in Figure 25, generated by visible light excitation, is in equilibrium with the almost isoenergetic lowest triplet excited state of the covalently linked pyrene moiety [29]. As a result, the lifetime of the excited photosensitizer becomes 2.5  $\mu\text{s}$  in deoxygenated acetonitrile at room temperature, i.e., more than three times longer than that of  $[\text{Ru}(\text{bpy})_3]^{2+}$  under the same conditions.

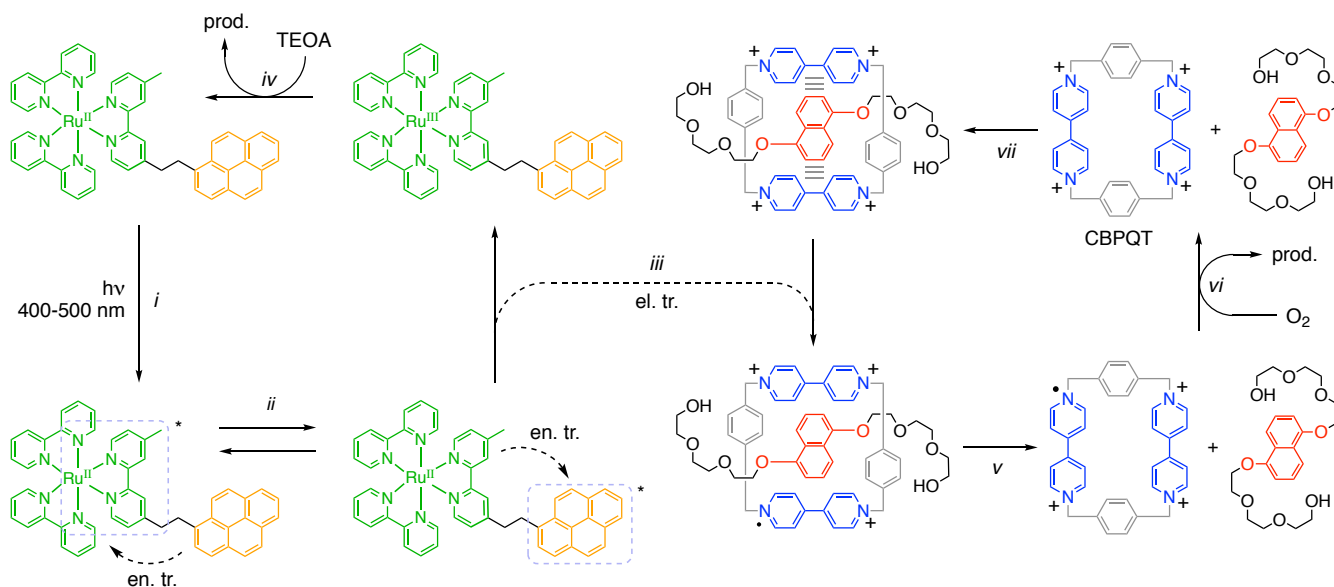


**Figure 25.** Mechanistic scheme of a molecular machine based on the photoinduced dethreading/rethreading of a pseudorotaxane by means of a Ru-pyrene bichromophoric photosensitizer, triethanolamine (TEOA) as a sacrificial reductant, and molecular oxygen as a sacrificial oxidant [92].

The photoinduced operation of the molecular machine is schematized in Figure 25. In deoxygenated acetonitrile at room temperature, visible light excitation of the metal complex (step *i*) produces a long-lived excited state, arising from equilibration of the Ru-centered and pyrene-centered triplet states (step *ii*). The photosensitizer is then quenched by the pseudorotaxane via oxidative electron transfer (step *iii*), and the formed Ru(III) complex is intercepted by triethanolamine (TEOA) used as a sacrificial reductant (step *iv*). CBPQT is permanently reduced, and its CT interaction with the naphthalene guest is turned off, thus promoting dethreading (step *v*). The cycle is closed by CBPQT reoxidation, caused by the dioxygen allowed to enter the solution (step *vi*), and subsequent reassembly of the pseudorotaxane

(step *vii*). The efficiency of the photoinduced dethreading was found to depend on the number of pyrene energy reservoirs appended to the Ru complex, and to increase on increasing the number of pyrene moieties.

A similar pseudorotaxane in which the molecular axle is non-symmetric (that is, oriented) was studied with the purpose of obtaining unidirectional threading and dethreading processes triggered by redox stimuli [93]. Light-driven operation, based on a photocatalytic cycle similar to that shown in Figure 25 with  $[\text{Ru}(\text{bpy})_3]^{2+}$  as a sensitizer, was also investigated. Other examples of photoinduced electron transfer involving Ru(II) polypyridine complexes and pseudorotaxanes [94, 95] or molecular tweezers [96, 97] have been reported in the past decade.

**Rotaxanes.** The discovery that the two-electron reduced form of CBPQT (Figure 25) yields strong inclusion complexes with 4,4'-bipyridinium radical cations in water [98], as a result of radical-radical interactions that occur between reduced bipyridinium compounds [99], has led to the development of novel mechanically interlocked species in which intercomponent interactions can be controlled by redox chemistry [100]. An example is provided by the [2]rotaxane shown in Figure 26, which features CBPQT as the macrocyclic ring, and an axle containing a  $[\text{Ru}(\text{bpy})_3]^{2+}$ -type stopper, and naphthalene and 4,4'-bipyridinium recognition sites [101].

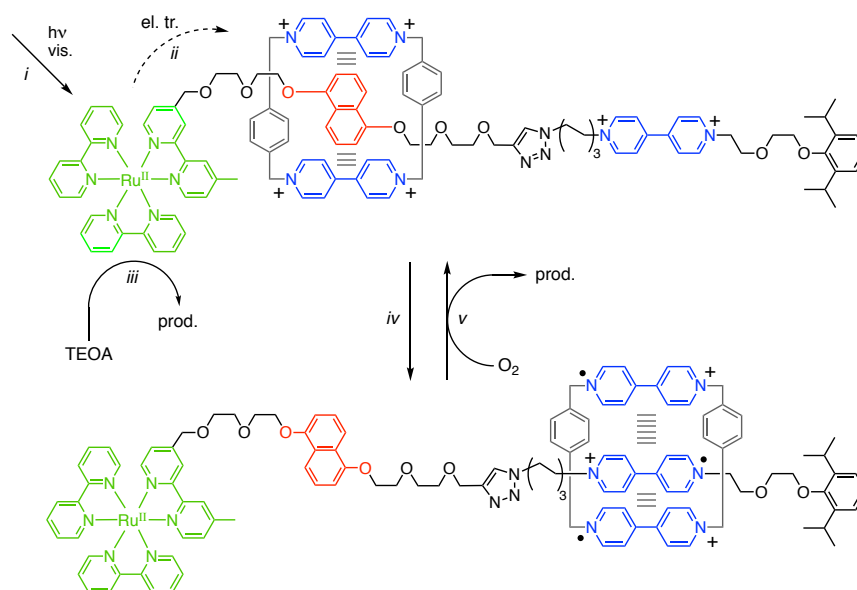


**Figure 26.** Structural formula and operation scheme of a molecular shuttle based on the photoinduced switching of charge-transfer and radical-radical interactions [101].

Spectroscopic ( $^1\text{H}$  NMR, UV-visible) and electrochemical measurements show that the CBPQT ring encircles the naphthalene electron-donating unit on account of CT interactions (Figure 26, top). Upon selective excitation of the Ru photosensitizer by visible light (step *i*), an electron is transferred intramolecularly to a bipyridinium unit of the ring or axle components (step *ii*) and, in the presence of the TEOA scavenger (step *iii*), becomes trapped. Prolonged irradiation eventually generates a rotaxane where all the three bipyridinium units are monoreduced (step *iv*); in this species, the bireduced CBPQT ring surrounds the monoreduced bipyridinium radical cation on the axle and interacts with it by radical pairing interactions (Figure 26, bottom). Subsequent reaction by  $\text{O}_2$  (air is allowed to enter the originally deoxygenated solution) affords the fully oxidized rotaxane, with concomitant return of CBPQT on the naphthalene site. Thus, the rotaxane behaves as a reversible molecular shuttle driven by optical and chemical stimuli.

It should be noted, however, that the strategy described in Figures 25 and 26 does not conduce to autonomous light-driven operation of the molecular device, because an operator-dependent sequence of photoinduced ‘forward’ and chemical ‘backward’ reactions has to be carried out. Moreover, these molecular machines consume chemical ‘fuels’ (TEOA and  $\text{O}_2$ ) besides light energy. A rotaxane that exhibits autonomous molecular shuttling driven exclusively by visible light is shown in Figure 27 [102, 103]. In this compound a  $\text{Ru}(\text{bpy})_3^{2+}$  stopper (P) is placed at the extremity of an axle component containing a rigid *p*-terphenyl spacer, and two  $\pi$ -electron acceptor units, namely a 4,4'-bipyridinium ( $\text{A}_1$ ) and its 3,3'-dimethyl analogue ( $\text{A}_2$ ). The macrocycle, a bis-*p*-phenylene-34-crown-10 (BPP34C10), is a  $\pi$ -electron donor and encircles the better electron-accepting site,  $\text{A}_1$ . Upon reduction of  $\text{A}_1$ , the ring moves and encircles the secondary recognition site  $\text{A}_2$ ; successive re-oxidation restores the initial position of the ring.

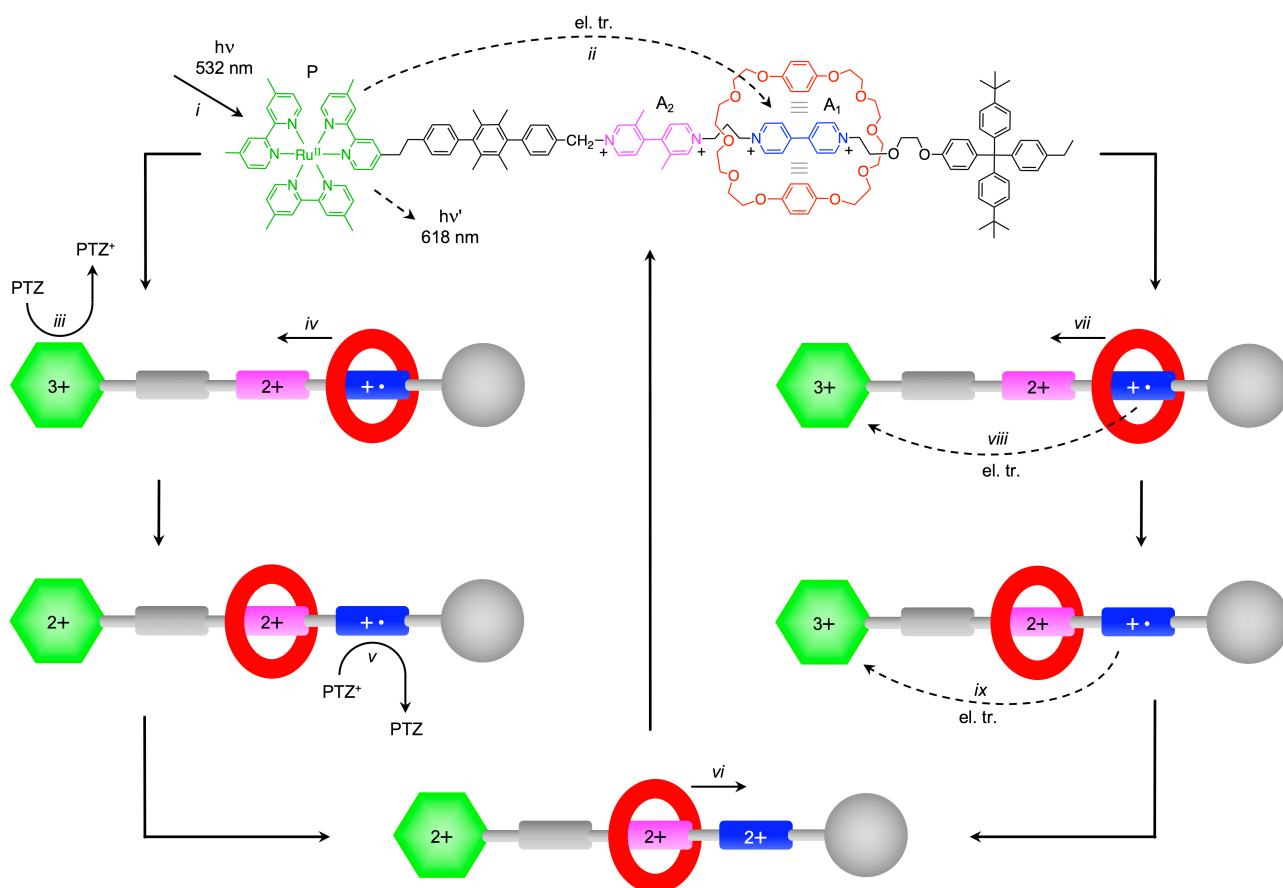


**Figure 27.** Structural formula of a rotaxane that can operate as an autonomous light-driven molecular shuttle, according to a mechanism that either involves bimolecular reactions with phenothiazine (PTZ) as an electron relay (left), or is based solely on intramolecular processes (right) [103].

The molecular shuttle can be operated by three different mechanisms, all of them involving the initial reduction of A<sub>1</sub> by electron transfer from the photoexcited Ru complex. In the sacrificial mechanism, already described in Figures 25 and 26 for related compounds, TEOA is employed to scavenge the photogenerated Ru(III) moiety, allowing the accumulation of the reduced A<sub>1</sub> species and causing the ring shuttling. Successive reaction with oxygen provides the reset of the machine. As discussed above, this approach does not lead to the exclusive and autonomous exploitation of the photons. A ‘photon-only’ autonomous mechanism is permitted by the use of phenothiazine (PTZ) as a reversible reductant in the place of TEOA (Figure 27, left) [103]. In this scheme, photoexcitation of P (step *i*) triggers an electron transfer to A<sub>1</sub> (step *ii*); because of the competition with the other inherent decay pathways of the P\* excited state – including its MLCT phosphorescence – the quantum yield is about 16%. The back electron transfer is prevented by phenothiazine, which quickly reacts with the oxidized photosensitizer

(step *iii*). The deactivation of the A<sub>1</sub> recognition site due to reduction causes the movement of the ring to encircle A<sub>2</sub> (step *iv*). The reaction between oxidized PTZ and reduced A<sub>1</sub> (step *v*), which is intermolecular and thus relatively slow, restores the electron acceptor power to the A<sub>1</sub> site; as a consequence, the thermally activated return of the macrocycle at the original position takes place (step *vi*).

Interestingly, the kinetic data (determined by a combination of electrochemical techniques and time-resolved absorption and luminescence spectroscopies) indicate that the reversible shuttling can also occur, with a lower efficiency, without the use of an external reductant [103]. The key issue of such a mechanism, based solely on intramolecular processes (Figure 27, right), is the competition between ring shuttling from reduced A<sub>1</sub> to A<sub>2</sub> (step *vii*) and back electron transfer from the reduced A<sub>1</sub> unit still encircled by the ring (step *viii*). In fact, in acetonitrile at 30 °C the back electron transfer is about 7 times faster than the motion of the macrocycle, leading to a ring shuttling efficiency of 12%. After electronic reset (step *ix*), the ring returns onto the initial site (step *vi*), thus completing a ‘four stroke’ sequence. The overall quantum yield for ring shuttling is  $16\% \times 12\% = 2\%$ .

The compound described in Figure 27 represents one of the most sophisticated examples of light-driven artificial molecular machines reported to date, and gathers together a number of unique features: 1) it is powered by visible light (i.e., sunlight); 2) it exploits its energy source autonomously; 3) it does not use chemical fuels and does not produce waste; 4) its working scheme relies only on intramolecular processes; 5) it can be cycled at high frequencies (up to 1 KHz); 6) it operates in mild conditions (fluid solution at ambient temperature), and; 7) it is very robust. The rotaxane was thoroughly studied computationally [104], and related compounds with inverted order of recognition sites [105], or different covalently [106] or non-covalently [107] linked Ru-based moieties were also investigated.

**Catenanes.** Molecular machines based on [2]catenanes exhibit the controlled pirouetting of one molecular ring with respect to the other, with continuous unidirectional rotation achieved in a few cases [74, 76-79]. Photoinduced ring pirouetting in the catenane shown in Figure 28 relies on a design identical to that of the rotaxane discussed in Figure 26 [108]. The system was investigated by spectroscopic (NMR, EPR, steady-state and time-resolved UV-vis absorption and luminescence) and electrochemical (voltammetry, spectroelectrochemistry) techniques. In the initial state the CBPQT-type ring surrounds the naphthalene electron-donating site of the other macrocycle by virtue of CT



interactions (Figure 28, top). In deoxygenated acetonitrile, selective excitation of the  $\text{Ru}[(\text{bpy})_3]^{2+}$  unit by visible light (step *i*) triggers an electron transfer to a bipyridinium unit (step *ii*); prolonged irradiation in the presence of TEOA (step *iii*) leads to reduction of all bipyridinium units in both molecular rings (step *iv*). In such a tris-radical cationic form, because of radical pairing interactions, the CBPQT-type ring encircles the bipyridinium radical cation of the other ring (Figure 28, bottom). By subsequent air bubbling, the radical cations are reoxidized by oxygen (step *v*) and the naphthalene site returns inside the CBPQT-type macrocycle, thus completing the switching cycle. It should be noted that since the two half-rotations caused by consecutive reduction and oxidation are not correlated, the catenane behaves as a mechanical switch and not as a rotary motor.

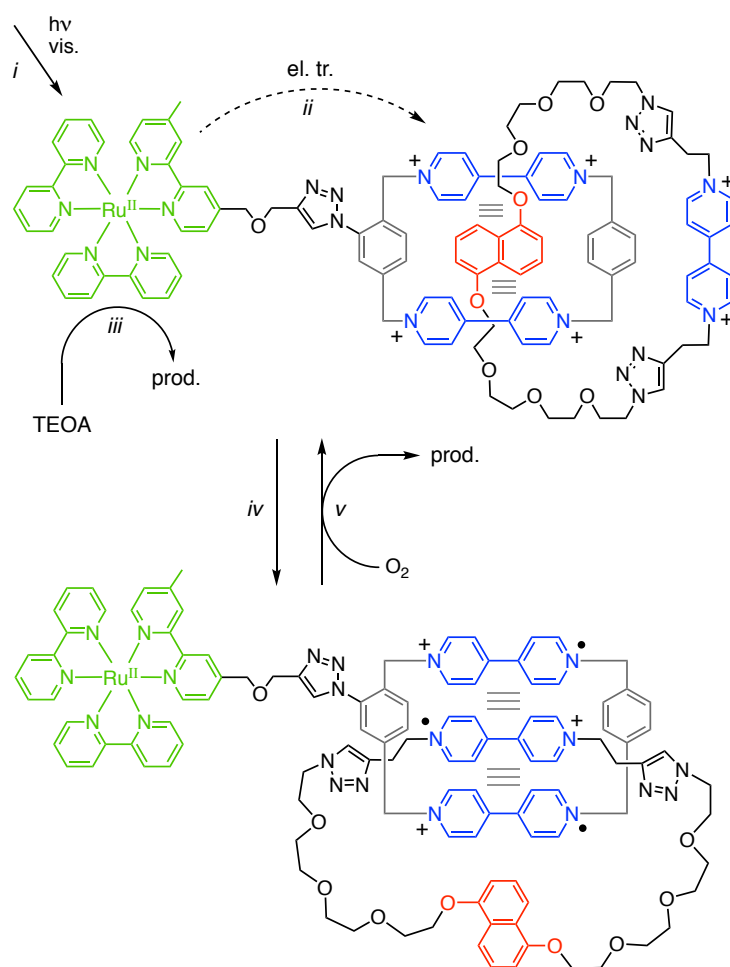


**Figure 28.** Structural formula and operation scheme of a catenane that exhibits ring pirouetting arising from the photoinduced modulation of charge-transfer and radical-radical interactions [108].

#### 4.4. Ligand photodissociation

Another family of molecular machines takes advantage of the dissociative character of ligand-field excited states of Ru(II)-diimine coordination compounds. As anticipated in Section 1.2, complexes that assume a distorted octahedral geometry exhibit a  $^3\text{MC}$  (d-d) excited state low enough in energy to be thermally populated from the lowest  $^3\text{MLCT}$  state which, in turn, can be generated by visible light excitation [6, 9]. Hence, irradiation of these complexes with visible light results in the expulsion of a ligand and its substitution by solvent molecules or other species such as anions (Figure 5a).

Two related mechanically interlocked structures, a [2]catenane [109] and a [2]rotaxane [110], where ligand photodissociation is exploited to trigger a mechanical movement of the molecular components, were synthesized and studied (Figure 29). Both compounds contain a macrocycle which comprises a 2,2'-bipyridine bidentate ligand, whereas the second component (either the other ring in the catenane or the axle in the rotaxane) incorporates two 1,10-phenanthroline units and thus behaves as a tetradentate chelate. In the interlocked structure, the Ru(II) center is coordinated to one bipyridine and two phenanthroline ligands which surround the metal in an octahedral geometry. Upon visible irradiation of either compound, in acetonitrile or in presence of a chloride salt, the bpy ligand is expelled from the complex and the corresponding macrocycle is detached from the other molecular component. This process leads to a rearrangement involving ring rotation in the catenane (Figure 29a) or shuttling in the rotaxane (Figure 29b), while the vacant sites at the metal center are filled by either acetonitrile molecules or chloride ions. Thermal recoordination of the bidentate chelate, with concomitant reset of the initial structure, takes place in the dark.

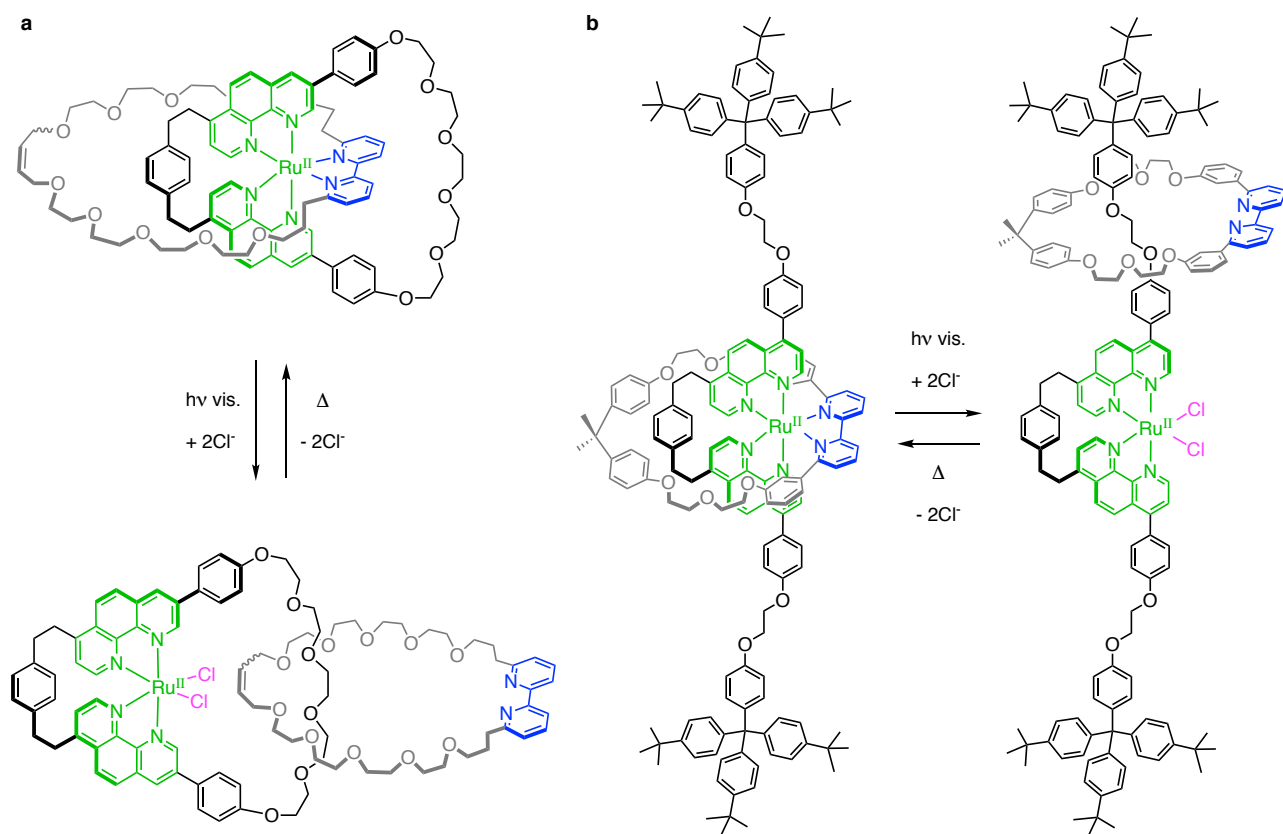
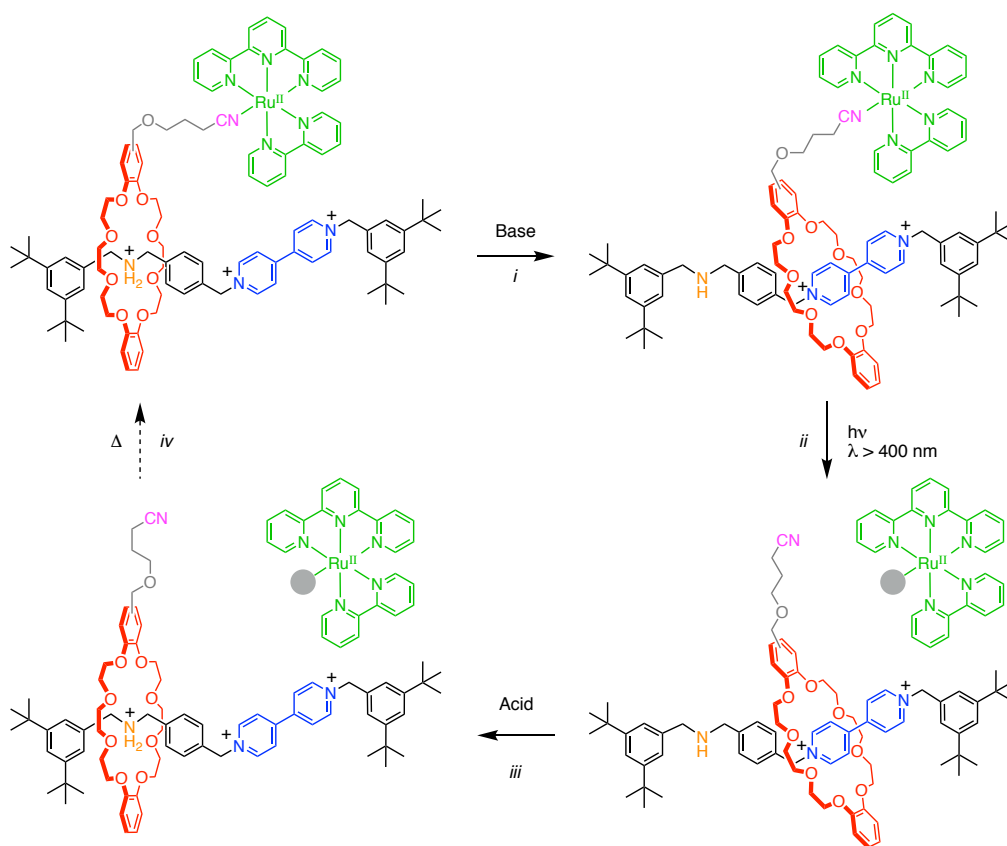


Figure 29. Structural formulas and mechanism of light-induced rearrangement in a catenane (a) and in a rotaxane (b) driven by ligand photodissociation in distorted octahedral Ru(II) complexes [109, 110].

More recently, a similar strategy was applied to design a molecular machine that possesses the structural and functional elements required to carry out controlled and directed transport of a molecular cargo at the nanoscale [111]. Since the controlled transport of substrates within cells is a key task of biomolecular machines [75], the development of artificial ‘molecular transporters’ is a fascinating challenge for nanoscience that can reveal new routes for several applications in technology and medicine [112].

The ‘transporter’ is a rotaxane-based shuttle whose ring component contains an anchoring site for the docking and undocking of a molecular cargo. As the translocation of the macrocycle and the release of the cargo should be controlled independently by non-interfering stimuli, orthogonal reactions need to be used to carry out the two processes. The rotaxane (Figure 30) is composed of a crown ether ring and a molecular axle comprising a dibenzylammonium and a 4,4’-bipyridinium recognition sites [111]. The macrocycle resides on the former unit, owing to hydrogen bonding, but it moves quantitatively and

reversibly around the latter with the addition of a base that switches off the ammonium site by deprotonation. Therefore, the motion of the ring can be controlled by acid/base stimuli. The crown ether is functionalized with a short chain ending with a nitrile group as a docking point for the cargo, which is a  $[\text{Ru}(\text{tpy})(\text{bpy})\text{L}]^{2+}$  complex (tpy is 2,2';6',2''-terpyridine and L is a monodentate ligand). The release of the cargo is controlled by the photochemical ligand decooordination reaction of Ru(II)-diimine complexes described above.



**Figure 30.** Structural formula and operation mechanism of a rotaxane-based molecular transporter. The ring transfer-return and cargo docking-undocking processes are the horizontal and vertical reactions, respectively. Grey circles represent nucleophilic molecules or ions present in solution which act as adventitious ligands [111].

The operation of the molecular transporter, observed by NMR-UV-visible spectroscopies and voltammetry, can be summarized as follows (Figure 30). In the initial state, the loaded macrocycle resides on the ammonium site; the addition of a base causes the transfer of the ring (and attached cargo) on the bipyridinium site (step *i*). At this point, irradiation with visible light induces the decoordination of the Ru(II) complex from the –CN link with release of the cargo (step *ii*); this reaction does not affect the position of the ring. The subsequent addition of an acid restores the initial position of the macrocycle (step *iii*) which, in principle, can be reloaded with another cargo (step *iv*). In practice, such a thermal docking occurs with a very little efficiency, most likely because the vacant position on the Ru center is filled with adventitious ligands that prevent the coordination of the –CN moiety of the rotaxane.

## 5. Conclusion

No doubt,  $[\text{Ru}(\text{bpy})_3]^{2+}$  has been and still is one of the most influential molecules in the development of chemistry in the last five decades. The first phase of such a development was characterized by the systematic exploration of the synthesis and properties of Ru(II) complexes with a variety of polypyridine-type ligands as well as of mixed ligand systems containing one or two bipyridine-type units. An exhaustive review [6] published in 1988 collects photochemical, photophysical, and redox data of several hundreds of Ru(II) polypyridine complexes. Then, with the development of supramolecular photochemistry [113],  $[\text{Ru}(\text{bpy})_3]^{2+}$  and its derivatives became fundamental building blocks for the construction of di-, tri-, tetra-, hexa-, deca- and docosa-nuclear complexes, both homo- and hetero-nuclear [114]. In an attempt to find molecules with even more interesting spectroscopic and redox properties than  $[\text{Ru}(\text{bpy})_3]^{2+}$ , luminescent cyclometalated complexes of Rh(III), Ir(III) and Pt(IV) complexes were obtained [115], but none of them has become popular as  $[\text{Ru}(\text{bpy})_3]^{2+}$ . With the development of molecular photonics,  $[\text{Ru}(\text{bpy})_3]^{2+}$  and related compounds were extensively used to perform energy- and electron-transfer processes in supramolecular systems (Section 2) including dendrimers (Section 3) [55]. As we have seen in Section 4, the complexes of the Ru-polypyridine family are extensively used to introduce light-induced functionalities in molecular machines [55]. In the last decade,  $[\text{Ru}(\text{bpy})_3]^{2+}$  and its derivatives have been widely used in photoredox catalysis: the Ru(II) complex absorbs visible light and promotes photoinduced electron transfer reactions [116] with

organic substrates, a metal-based catalyst, or sacrificial reagents to drive organic reactions under mild experimental conditions. The use of  $[\text{Ru}(\text{bpy})_3]^{2+}$  in debromination reactions [117] and in Pschorr cyclizations [118] dates back to 1984, but its renaissance started in 2008 with the publication of a seminal paper by MacMillan [119], merging organocatalysis and photocatalysis. Moreover, some derivatives of  $[\text{Ru}(\text{bpy})_3]^{2+}$ , ad hoc prepared, have been extensively used for biological purposes as probes of biological sites, as well as photocleavage agents and inhibitors of biological functions [120, 121, 122], thereby adding a further dimension to the applications of this unique metal complex.

As described in this review,  $[\text{Ru}(\text{bpy})_3]^{2+}$  complex and its derivatives are still unrivalled in many fields of applications because of their exceptional photophysical and redox properties coupled to chemical and photochemical stability. However, there are some drawbacks related to specific applications, such as poor absorption in the red region of the visible spectrum, presence of a heavy and rare metal ion. We envision that future efforts will be devoted to solve these drawbacks by the study of alternatives metal complexes or organic dyes.

**Acknowledgment.** This work was supported by the Italian Ministry of University and Research (grants FARE R16S9XXKX3 and PRIN 20173L7W8K) and the University of Bologna.

## 6. References

- [1] V. Balzani, V. Carassiti, *Photochemistry of Coordination Compounds*, Academic Press, London, 1970.
- [2] C. Costentin, M. Robert, J.-M. Savéant, C. Tard, *Acc. Chem. Res.* 47 (2014) 271–280.
- [3] V. Balzani, P. Ceroni, A. Juris, *Photochemistry and Photophysics: Concepts, Research, Applications*, Wiley, Weinheim 2014.
- [4] V. Balzani, A. Juris, *Coord. Chem. Rev.* 211 (2001) 97-115.
- [5] V. Balzani, G. Bergamini, P. Ceroni, *Angew. Chem. Int. Ed.* 54 (2015) 11320–11337.
- [6] A. Juris, V. Balzani, F. Barigelletti, S. Campagna, P. Belser, A. von Zelewsky, *Coord. Chem. Rev.* 84 (1988) 85-277.
- [7] K. Kalyanasundaram, *Photochemistry of Polypyridine and Porphyrin Complexes*, Academic Press, London, 1992.
- [8] V. Balzani, G. Bergamini, P. Ceroni, *Rend. Fis. Acc. Lincei* 28(1) (2017) 125-142.

- [9] S. Campagna, F. Puntoriero, F. Nastasi, G. Bergamini, V. Balzani, *Top. Curr. Chem.* 280 (2007) 117-214.
- [10] G.A. Crosby, *Acc. Chem. Res.* 8 (1975) 231-238.
- [11] G. Ciamician, *Bull. Soc. Chim. Fr.* 3 (1908) 1-18.
- [12] L. Pause, M. Robert, J.M. Saveant, *J. Am. Chem. Soc.* 121 (1999) 7158-7159.
- [13] S. Roffia, R. Casadei, F. Paolucci, C. Paradisi, C. A. Bignozzi, F. Scandola, *J. Electroanal. Chem.* 302 (1991) 157-171.
- [14] R. Ballardini, V. Balzani, A. Credi, M. T. Gandolfi, M. Venturi, *Int. J. Photoenergy* 3 (2001) 63-77.
- [15] G.A. Crosby, D.M. Klassen, *J. Chem. Phys.* 48 (1968) 1853-1857.
- [16] V. Balzani, F. Bolletta, M. Ciano, M. Maestri, *J. Chem. Educ.* 60 (1983) 447-450.
- [17] A.J. Bard (Ed.), *Electrogenerated Chemiluminescence*, Marcel Dekker, New York, 2004.
- [18] F. Bolletta, V. Balzani, *J. Am. Chem. Soc.* 104 (1982) 4250-4251.
- [19] P. Ceroni, G. Bergamini, V. Balzani, *Angew. Chem. Int. Ed.* 48 (2009) 8516-8518.
- [20] B. Schlicke, P. Belser, L. De Cola, E. Sabbioni and V. Balzani, *J. Am. Chem. Soc.*, 121 (1999) 4207-4214.
- [21] S. Welter, N. Salluce, P. Belser, M. Groeneveld, L. De Cola, *Coord. Chem. Rev.* 249 (2005) 1360-1371.
- [22] S. Welter, F. Lafolet, E. Cecchetto, F. Vergeer, L. De Cola, *ChemPhysChem.* 6 (2005) 2417-2427.
- [23] M.T. Indelli, C. Chiorboli, L. Flamigni, L. De Cola, F. Scandola, *Inorg. Chem.* 46 (2007) 5630-5641.
- [24] M. Natali, S. Campagna, F. Scandola, *Chem. Soc. Rev.* 43 (2014) 4005-4018.
- [25] M. Venturi, F. Marchioni, B. Ferrer, V. Balzani, D. M. Opris, A. D. Schlüter, *ChemPhysChem*, 7 (2006), 229-239.
- [26] M. Venturi, F. Marchioni, V. Balzani, D.M. Opris, O. Henze, A.D. Schlüter, *Eur. J. Org. Chem.*, (2003) 4227-4233.
- [27] P. Belser, R. Dux, M. Baak, L. De Cola and V. Balzani, *Angew. Chem. Int. Ed. Engl.*, 34 (1995) 595-598.
- [28] L. De Cola, V. Balzani, P. Belser, R. Dux and M. Baak, *Supramol. Chem.*, 5 (1995) 297-299.
- [29] W.E. Ford, M.A.J. Rodgers, *J. Phys. Chem.* 96 (1992) 2917-2920.
- [30] N.D. McClenaghan, F. Barigelletti, B. Maubert and S. Campagna, *Chem. Commun.* (2002) 602-603.
- [31] P. Manca, M. I. Pilo, G. Sanna, A. Zucca, G. Bergamini and P. Ceroni, *Chem. Commun.*, 47 (2011), 3413-3415.
- [32] J.-P. Sauvage, J.-P. Collin, J.-C. Chambron, S. Guillerez, C. Coudret, V. Balzani, F. Barigelletti, L. De Cola and L. Flamigni, *Chem. Rev.*, 1994, 94, 993-1019.
- [33] N. Armaroli, *ChemPhysChem.* 9 (2008) 371-373.
- [34] A. Lavie-Cambot, C. Lincheneau, M. Cantuel, Y. Leydet, N.D. McClenaghan, *Chem. Soc. Rev.* 39 (2010) 506-515.
- [35] Jiang, J. Peng, J. Wang, X. Guo, D. Zhao, Y. Ma, *ACS Appl. Mater. Interfaces.* 8 (2016) 3591-3600.
- [36] S.A. Denisov, Q. Gan, X. Wang, L. Scarpantonio, Y. Ferrand, B. Kauffmann, G. Jonusauskas, I. Huc, N.D. McClenaghan, *Angew. Chemie.* 128 (2016) 1350-1355.
- [37] Q. Chen, Y. Liu, X. Guo, J. Peng, S. Garakyaraghi, C.M. Papa, F.N. Castellano, D. Zhao, Y. Ma, *J. Phys. Chem. A.* 122 (2018) 6673-6682.

- [38] (a) S. Campagna, P. Ceroni, F. Puntoriero (Eds.), *Designing Dendrimers*, John Wiley & Sons, Hoboken, 2012; (b) F. Vögtle, G. Richardt, N. Werner, *Dendrimer Chemistry*, Wiley-VCH, Weinheim, 2009; (c) J. M. J. Fréchet, D. A. Tomalia (Eds.), *Dendrimers and Other Dendritic Polymers*, John Wiley & Sons, Chichester, 2001; (d) G. R. Newkome, F. Vögtle, *Dendrimers and Dendrons*, Wiley-VCH, Weinheim, 2001.
- [39] For some reviews, see: (a) M. Gingras, J.-M. Raimundo, Y. M. Chabre, *Angew. Chem. Int. Ed.* 46 (2007) 1010-1017; (b) C. A. Schalley, B. Baytekin, H. T. Baytekin, M. Engeser, T. Felder, A. Rang, *J. Phys. Org. Chem.* 19 (2006) 479-490; (c) T. Darbre, J.-L. Reymond, *Acc. Chem. Res.* 39 (2006) 925-934; (d) D. Astruc, F. Chardac, *Chem. Rev.* 101 (2001) 2991-3024; (e) M. W. P. L. Baars, E. W. Meijer, *Top. Cur. Chem.* 210 (2000) 131-182.
- [40] A.-M. Caminade, C. O. Turrin, R. Laurent, A. Ouali, B. Delavaux-Nicot, *Dendrimers: Towards Catalytic, Material and Biomedical Uses*, Wiley, Chichester, 2011.
- [41] For some reviews, see: (a) G. Bergamini, E. Marchi, P. Ceroni, *Coord. Chem. Rev.* 255 (2011) 2458-2468; (b) D. Astruc, E. Boisselier, C. Orneals, *Chem. Rev.* 110 (2010) 1857-1959; (c) R. Deloncle, A.-M. Caminade, *J. Photochem. Photobiol. C* 11 (2010) 25-45; (d) W.-S. Li, T. Aida, *Chem. Rev.* 109 (2009) 6047-6076.
- [42] For some examples, see e.g.: (a) M. Shelliah, Y. C. Rajan, H.-C. Lin, *J. Mater. Chem.* 22 (2012) 8976-8987; (b) J. Yang, S. Lee, H. Lee, J. Lee, H. K. Kim, S. U. Lee, D. Sohn, *Langmuir* 27 (2011) 8898-8904; (c) Y. Ochi, A. Fujii, R. Nakajima, K. Yamamoto, *Macromolecules* 43 (2010) 6570-6576; (d) B. Branchi, P. Ceroni, V. Balzani, F.-G. Klaerner, F. Vögtle, *Chem. Eur. J.* 16 (2010) 6048-6055.
- [43] (a) S.-H. Hwang, C. D. Shreiner, C. N. Moorefield, G. R. Newkome, *New J. Chem.* 31 (2007) 1192-1217; (b) P. Ceroni, G. Bergamini, F. Marchioni, V. Balzani, *Prog. Polym. Sci.* 30 (2005) 453-473.
- [44] A. E. Kaifer, *Eur. J. Inorg. Chem.* (2007) 5015-5027.
- [45] (a) F. Puntoriero, G. Bergamini, P. Ceroni, V. Balzani, F. Vögtle, *New J. Chem.* 32 (2008) 401-406; (b) G. Ramakrishna, A. Bhaskar, P. Bauerle, T. Goodson III, *J. Phys. Chem. A* 112 (2008) 2018-2026; (c) D. Cao, S. Dobis, C. Gao, S. Hillmann, H. Meier, *Chem. Eur. J.* 13 (2007) 9317-9323.
- [46] V. Balzani, G. Bergamini, P. Ceroni, E. Marchi, *New J. Chem.* 35 (2011) 1944-1954.
- [47] D. Astruc, C. Ornelas, J. Ruiz, *Acc. Chem. Res.* 41 (2008) 841-856.
- [48] P. A. Chase, R. J. M. K. Gebbink, G. van Koten, *J. Organomet. Chem.* 689 (2004) 4016-4054.
- [49] D. K. Smith, F. Diederich, *Top. Curr. Chem.* 210 (2000) 183-227.
- [50] V. Balzani, S. Campagna, G. Denti, A. Juris, S. Serroni, M. Venturi, *Acc. Chem. Res.* 31 (1998) 26-34.
- [51] H. D. Abruña, *Anal. Chem.* 76 (2004) 310A-319A.
- [52] N. Nishide, K. Oyaizu, *Science* 319 (2008) 737-738.
- [53] F. Vögtle, M. Plevoets, M. Nieger, G. C. Azzellini, A. Credi, L. De Cola, V. De Marchis, M. Venturi, V. Balzani, *J. Am. Chem. Soc.* 121 (1999) 6290-6298.
- [54] V. Balzani, P. Ceroni, M. Maestri, V. Vicinelli, *Curr. Opin. Chem. Biol.* 7 (2003) 657-665.
- [55] V. Balzani, A. Credi, M. Venturi, *Molecular Devices and Machines – Concepts and Perspectives for the Nano World*, Wiley-VCH, Weinheim, 2008, pp. 132-173.
- [56] M. Plevoets, F. Vögtle, L. De Cola, V. Balzani, *New J. Chem.* 23 (1999) 63-69.
- [57] For some reviews, see: (a) P. Ceroni, *Chem. Eur. J.* 17 (2011) 9560-9564; (b) T. N. Singh-Rachford, F. N. Castellano, *Coord. Chem. Rev.* 254 (2010) 2560-2573.
- [58] G. Bergamini, P. Ceroni, P. Fabbri, S. Cicchi, *Chem. Commun.* 47 (2011) 12780-12782.



- [59] (a) M. Venturi, P. Ceroni, *Curr. Top. Electrochem.* 16 (2011) 31-45; (b) P. Ceroni, M. Venturi in *Electrochemistry of Functional Supramolecular Systems* (P. Ceroni, A. Credi, M. Venturi, Eds.), Wiley, Hoboken, 2010, pp. 145-184.
- [60] D. Astruc, C. Ornelas, J. Ruiz, *Chem. Eur. J.* 15 (2009) 8936-8944.
- [61] (a) J. I. Goldsmith, K. Takada, H. D. Abruña, *J. Phys. Chem. B* 106 (2002) 8504-8513; (b) C. Amatore, Y. Bouret, E. Maisonhaute, J. I. Goldsmith, H. D. Abruña, *ChemPhysChem* 2 (2001) 130-134; (c) C. Amatore, Y. Bouret, E. Maisonhaute, J. I. Goldsmith, H. D. Abruña, *Chem. Eur. J.* 7 (2001) 2206-2226; (d) G. D. Storrer, K. Takada, H. D. Abruña, *Langmuir* 15 (1999) 872-884.
- [62] L. Ravotto, R. Mazzaro, M. Natali, L. Ortolani, V. Morandi, P. Ceroni, G. Bergamini, *J. Phys. Chem. Lett.* 5 (2014) 798-803.
- [63] (a) L. M. Bronstein, Z. B. Shifrina, *Chem. Rev.* 111 (2011) 5301-5344; (b) R. M. Crooks, M. Zhao, L. Sun, V. Chechik, L. K. Yeung, *Acc. Chem. Res.* 34 (2001) 181-190; (c) D. Yamamoto, S. Watanabe, M. T. Miyahara, *Langmuir* 26 (2010) 2339-2345.
- [64] V. Balzani, L. Moggi, M. F. Manfrin, F. Bolletta, M. Gleria, *Science* 189 (1975) 852-856.
- [65] See, for example: (a) A. Fihri, V. Artero, M. Razavet, C. Baffert, W. Leibl, M. Fontecave, *Angew. Chem. Int. Ed.* 47 (2008) 564-567; (b) M. Elvington, J. Brown, S. M. Arachchige, K. Brewer, *J. Am. Chem. Soc.* 129 (2007) 10644-10645; (c) S. Rau, B. Schafer, D. Gleich, E. Anders, M. Rudolph, M. Friedrich, H. Görls, W. Henry, J. G. Vos, *Angew. Chem. Int. Ed.* 45 (2006) 6215-6218; (d) H. Ozawa, M. Haga, K. Sakai, *J. Am. Chem. Soc.* 128 (2006) 4926-4927.
- [66] G. Denti, S. Serroni, S. Campagna, A. Juris, M. Ciano, V. Balzani in *Perspectives in Coordination Chemistry* (A. F. Williams, C. Floriani, A. E. Merbach, Eds.), VCH, Basel, 1992, p. 153-164.
- [67] (a) F. Puntoriero, S. Serroni, G. La Ganga, A. Santoro, M. Galletta, F. Nastasi, E. La Mazza, A. M. Cancelliere, S. Campagna, *Eur. J. Inorg. Chem.* (2018) 3887-3899; (b) V. Balzani, P. Ceroni, A. Juris, M. Venturi, S. Campagna, F. Puntoriero, S. Serroni, *Coord. Chem. Rev.* 219 (2001) 545-572.
- [68] S. Campagna, G. Denti, S. Serroni, A. Juris, M. Venturi, V. Ricevuto, V. Balzani, *Chem. Eur. J.* 1 (1995) 207-268.
- [69] S. Roffia, M. Marcaccio, C. Paradisi, F. Paolucci, V. Balzani, G. Denti, S. Serroni, S. Campagna, *Inorg. Chem.* 32 (1993) 3003-3009.
- [70] For a decanuclear dendrimer of this family the oxidation of all the 10 component units was observed working in liquid SO<sub>2</sub>, that enables to explore a wide potential window. See: P. Ceroni, F. Paolucci, C. Paradisi, A. Juris, S. Roffia, S. Serroni, S. Campagna, A. J. Bard, *J. Am. Chem. Soc.* 120 (1998) 5480-5487.
- [71] F. Puntoriero, G. La Ganga, A. Sartorel, M. Carraro, G. Scorrano, M. Bonchio, S. Campagna, *Chem. Commun.* 46 (2010) 4725-4727.
- [72] (a) G. Denti, S. Campagna, S. Serroni, M. Ciano, V. Balzani, *J. Am. Chem. Soc.* 114 (1992) 2944-2950; (b) S. Serroni, A. Juris, M. Venturi, S. Campagna, I. Resino Resino, G. Denti, A. Credi, V. Balzani, *J. Mater. Chem.* 7 (1997) 1227-1236.
- [73] G. Bergamini, C. Saudan, P. Ceroni, M. Maestri, V. Balzani, M. Gorka, S.-K. Lee, J. van Heyst, F. Vögtle, *J. Am. Chem. Soc.* 126 (2004) 16466-164781.
- [74] V. Balzani, A. Credi, M. Venturi, *Molecular Devices and Machines, 2nd Ed.*, Wiley-VCH, Weinheim, 2008.
- [75] R. A. L. Jones, *Soft Machines – Nanotechnology and Life*, Oxford University Press, Oxford, 2008.
- [76] V. Balzani, A. Credi, F. M. Raymo, J. F. Stoddart, *Angew. Chem. Int. Ed.* 39 (2000) 3349-3391.
- [77] S. Erbas-Cakmak, D. A. Leigh, C. T. McTernan, A. L. Nussbaumer, *Chem. Rev.* 115 (2015) 10081-10206.

- [78] S. Kassem, T. van Leeuwen, A. S. Lubbe, M. R. Wilson, B. L. Feringa, D. A. Leigh, *Chem. Soc. Rev.* 46 (2017) 2592-2621.
- [79] C. Pezzato, C. Cheng, J. F. Stoddart, R. D. Astumian, *Chem. Soc. Rev.* 46 (2017) 5491-5507.
- [80] J. Groppi, M. Baroncini, M. Venturi, S. Silvi, A. Credi, *Chem. Commun.* 2019, 55, 12595-12602.
- [81] B. L. Feringa, *Angew. Chem. Int. Ed.* 56 (2017) 11060-11078.
- [82] J.-P. Sauvage, *Angew. Chem. Int. Ed.* 56 (2017) 11080-11093.
- [83] J. F. Stoddart, *Angew. Chem. Int. Ed.* 56 (2017) 11094-11125.
- [84] D. Dattler, G. Fuks, J. Heiser, E. Moulin, A. Perrot, X. Yao, N. Giuseppone, *Chem. Rev.* 120 (2020) 310-433.
- [85] S. Corra, M. Curcio, M. Baroncini, S. Silvi, A. Credi, *Adv. Mater.* 32 (2020) 1906064.
- [86] P. Ceroni, A. Credi, M. Venturi, *Chem. Soc. Rev.* 43 (2014) 4068-4083.
- [87] B. Colasson, A. Credi, G. Ragazzon, *Coord. Chem. Rev.* 325 (2016) 125-134.
- [88] S. J. Wezenberg, K.-Y. Chen, B. L. Feringa, *Angew. Chem. Int. Ed.* 54 (2015) 11457-11461.
- [89] P. R. Ashton, R. Ballardini, V. Balzani, S. E. Boyd, A. Credi, M. T. Gandolfi, M. Gomez-Lopez, S. Iqbal, D. Philp, J. A. Preece, L. Prodi, H. G. Ricketts, J. F. Stoddart, M. S. Tolley, M. Venturi, A. J. P. White, D. J. Williams, *Chem. Eur. J.* 3 (1997) 152-170.
- [90] P. R. Ashton, V. Balzani, A. Credi, O. Kocian, D. Pasini, L. Prodi, N. Spencer, J. F. Stoddart, M. S. Tolley, M. Venturi, A. J. P. White, D. J. Williams, *Chem. Eur. J.* 4 (1998) 590-607.
- [91] P. R. Ashton, R. Ballardini, V. Balzani, E. C. Constable, A. Credi, O. Kocian, S. J. Langford, J. A. Preece, L. Prodi, E. R. Schofield, N. Spencer, J. F. Stoddart, S. Wenger, *Chem. Eur. J.* 4 (1998) 2411-2422.
- [92] L. Scarpantonio, A. Tron, C. Destribats, P. Godard, N. D. McClenaghan, *Chem. Commun.* 48 (2012) 3981-3983.
- [93] H. Li, C. Cheng, P. R. McGonigal, A. C. Fahrenbach, M. Frasconi, W.-G. Liu, Z. Zhu, Y. Zhao, C. Ke, J. Lei, R. M. Young, S. M. Dyar, D. T. Co, Y.-W. Yang, Y. Y. Botros, W. A. Goddard III, M. R. Wasielewski, R. D. Astumian, J. F. Stoddart, *J. Am. Chem. Soc.* 135 (2013) 18609-18620.
- [94] T. K. Monhaphol, S. Andersson, L. Sun, *Chem. Eur. J.* 17 (2011) 11604-11612.
- [95] M. Semeraro, A. Secchi, S. Silvi, M. Venturi, A. Arduini, A. Credi, *Inorg. Chim. Acta* 417 (2014) 258-262.
- [96] C. Gao, S. Silvi, X. Ma, H. Tian, M. Venturi, A. Credi, *Chem. Commun.* 48 (2012) 7577-7579.
- [97] C. Gao, S. Silvi, X. Ma, H. Tian, A. Credi, M. Venturi, *Chem. Eur. J.* 18 (2012) 16911-16921.
- [98] A. Trabolsi, N. Khashab, A. C. Fahrenbach, D. C. Friedman, M. T. Colvin, K. K. Coti, D. Benitez, E. Tkatchouk, J.-C. Olsen, M. E. Belowich, R. Carmielli, H. A. Khatib, W. A. Goddard III, M. R. Wasielewski, J. F. Stoddart, *Nat. Chem.* 2 (2010) 42-49.
- [99] P. M. S. Monk, *The Viologens: physicochemical properties, synthesis and applications of the salts of 4,4'-bipyridine*, Wiley, Chichester, 1998.
- [100] Y. Wang, M. Frasconi, J. F. Stoddart, *ACS Cent. Sci.* 3 (2017) 927-935.
- [101] H. Li, A. C. Fahrenbach, A. Coskun, Z. Zhu, G. Barin, Y.-L. Zhao, Y. Y. Botros, J.-P. Sauvage, J. F. Stoddart, *Angew. Chem. Int. Ed.* 50 (2011) 6782-6788.
- [102] P. R. Ashton, R. Ballardini, V. Balzani, A. Credi, K. R. Dress, E. Ishow, C. J. Kleverlaan, O. Kocian, J. A. Preece, N. Spencer, J. F. Stoddart, M. Venturi, S. Wenger, *Chem. Eur. J.* 6 (2000) 3558-3574.

- [103] V. Balzani, M. Clemente-Leon, A. Credi, B. Ferrer, M. Venturi, A. H. Flood, J. F. Stoddart, *Proc. Natl. Acad. Sci. U. S. A.* 103 (2006) 1178-1183.
- [104] P. Raiteri, G. Bussi, C. S. Cucinotta, A. Credi, J. F. Stoddart, M. Parrinello, *Angew. Chem. Int. Ed.* 47 (2008) 3536-3539.
- [105] V. Balzani, M. Clemente-Leon, A. Credi, M. Semeraro, M. Venturi, H.-R. Tseng, S. Wenger, S. Saha, J. F. Stoddart, *Aust. J. Chem.* 59 (2006) 193-206.
- [106] G. J. E. Davidson, S. J. Loeb, P. Passaniti, S. Silvi, A. Credi, *Chem. Eur. J.* 12 (2006) 3233-3242.
- [107] B. Ferrer, G. Rogez, A. Credi, R. Ballardini, M. T. Gandolfi, V. Balzani, Y. Liu, H.-R. Tseng, J. F. Stoddart, *Proc. Natl. Acad. Sci. U. S. A.* 103 (2006) 18411-18416.
- [108] J. Sun, Y. Wu, Z. Liu, D. Cao, Y. Wang, C. Cheng, D. Chen, M. R. Wasielewski, J. F. Stoddart, *J. Phys. Chem. A* 119 (2015) 6317-6325.
- [109] P. Mobian, J.-M. Kern, J.-P. Sauvage, *Angew. Chem. Int. Ed.* 43 (2004) 2392-2395.
- [110] J.-P. Collin, D. Jouvenot, M. Koizumi, J.-P. Sauvage, *Eur. J. Inorg. Chem.* (2005) 1850-1855.
- [111] C. Schäfer, G. Ragazzon, B. Colasson, M. La Rosa, S. Silvi, A. Credi, *ChemistryOpen* 5 (2016) 120-124.
- [112] A. Credi, *Angew. Chem. Int. Ed.* 58 (2019) 4108-4110.
- [113] V. Balzani, F. Scandola, *Supramolecular Photochemistry*, Ellis Horwood, Chichester, England, 1991, pp. 425.
- [114] V. Balzani, A. Juris, M. Venturi, S. Campagna, S. Serroni, *Chem. Rev.* 96 (1996) 759-834.
- [115] M. Maestri, V. Balzani, C. Deuschel-Cornioley, A. von Zelewsky, *Adv. Photochem.* 17 (1992) 1-68.
- [116] For a recent example from our laboratory, see: A. Gualandi, G. Rodeghiero, A. Faraone, F. Patuzzo, M. Marchini, F. Calogero, R. Perciaccante, T. P. Jansen, P. Ceroni, P. G. Cozzi, *Chem. Commun.* 55 (2019) 838-6841.
- [117] R. Maidan, Z. Goren, J.Y. Becker, I. Willner, *J. Am. Chem. Soc.* 106 (1984) 6217-6222.
- [118] H. Cano-Yelo, A. Deronzier, *J. Chem. Soc., Perkin Trans. 2* (1984) 1093-1098.
- [119] D. A. Nicewicz, D. W. C. MacMillan, *Science* 322 (2008) 77-80.
- [120] V. Balzani, G. Bergamini, S. Campagna, F. Puntoriero, *Top. Curr. Chem.* 280 (2007) 1-36.
- [121] N. Soliman, G. Gasser, C. M. Thomas, *Adv. Mater.* (2020), DOI: 10.1002/adma.202003294
- [122] L. Jiang, X. Liu, L. Tanc, *J. Inorg. Biochem.* 213 (2020) 111263.

**This document is the unedited Author's version of a Submitted Work that was subsequently accepted for publication in *Coordination Chemistry Reviews*, copyright © Elsevier after peer review.**

**To access the final edited and published work, see:**

**<https://www.sciencedirect.com/science/article/abs/pii/S0010854520312091>**